Coordination Chemistry Reviews, 12 (1974) 1–35

BINUCLEAR OXO-BRIDGED IRON(III) COMPLEXES

K.S. MURRAY

Chemistry Department, Monash University, Clayton, Victoria 3168 (Australia)

(Received March 27th, 1973)

CONTENTS

A. INTRODUCTION

Though binuclear oxo-bridged* iron(III) complexes constitute only one example of a general class of oxo-bridged metal species, their preparation and properties are reviewed here for a number of reasons; (a) they allow detailed study, by modern physicochemical, spectroscopic and structural techniques, of magnetic-exchange interactions in a system with spin much higher than that commonly encountered; (b) they give insight into aspects of the hydrolysis of iron(III); (c) they are model compounds for some biologically important haemerythrin and haem protein systems.

Certain aspects of the present account are covered more generally in recent reviews of the following subjects: oxo-bridging in polynuclear complexes[1–3]; coordination chemistry of iron(III)[4]; magnetic exchange interactions in polynuclear complexes[5–9]; biological implications of polynuclear iron complexes[10–12]. Gray[13] has written a short review of some aspects of the oxo-bridged iron(III) HEDTA system and its possible biological relevance.

(i) Historical aspects

The first oxo-bridged iron(III) complex to be prepared was the Schiff-base derivative (Fe salen)$_2$O. Pfeiffer et al.[14] were able to formulate correctly the structure of this complex in 1933 without the aid of spectroscopic and structural instrumentation. Shortly afterwards the phenanthroline dimers were prepared but formulated as having a di-hydroxo bridge[15]. Anomalously low magnetic moments were first observed for iron(III) complexes in the early thirties and were ascribed to binuclear species with oxo or di-hydroxo bridging (ref. 15, 17). It was not until the work of Lewis and co-workers in the sixties[18–20], however, that the currently accepted description of the magnetic behaviour was forthcoming. They put forward a general model of antiferromagnetic exchange between two high-spin ($S = \frac{5}{2}$) iron(III) centres. Furthermore, all complexes of this type, isolated in the crystalline state, were thought[21] to possess a single $(Fe{-}O{-}Fe)^{4+}$ bridge rather than the diol alternative $(Fe(OH)_2Fe)^{4+}$ and a large amount of detailed spectroscopic, magnetic and X-ray crystallographic work has been carried out recently, based on and confirming the model of Lewis et al.

The observations of inorganic chemists on the "simple" oxo-bridged iron(III) complexes have subsequently been recognised and appreciated in more biologically oriented studies, and have helped in elucidating the structure of the active site in certain iron–protein systems.

(ii) Range of complexes and abbreviations

μ-Oxo iron(III) complexes have so far been isolated with chelating ligands which possess N donor or N, O donor atoms. The unidentate ligands Cl and H_2O can also coordinate to the iron atoms in the presence of chelating ligands.

---

* μ-oxo is the generally used nomenclature.

N donor atoms:

$[(Fe\ phen_2)_2O]^{4+}$	ref. 15, 18, 21–28
$[(Fe\ phen_2Cl)_2O]^{2+}$	ref. 21, 29
$[(Fe\ bipy_2)_2O]^{4+}$	ref. 21, 27, 28
$[(Fe\ terpy)_2O]^{4+}$	ref. 27
$(Fe\ porphyrin)_2O$	ref. 30–33
$[(Fe\ TAAB)_2O]^{4+}$	ref. 34

N, O donor atoms:

$(Fe\ salen)_2O$	and related ligands with different substitutions on the salicylaldehyde ring or the N–C–C–N bridge. ref. 14, 16, 19, 20
$[Fe(sal\text{-}NR)_2]_2O$	ref. 35
$[(Fe\ HEDTA)_2O]^{2-}$	ref. 36–38
$[(Fe\ EDTA)_2O]^{4-}$	ref. 36–38
$[(Fe\ B(H_2O))_2O]^{4+}$	ref. 39

The structures of the attached ligands and their abbreviations are shown in Fig.1.

B. SYNTHESIS

Two classes of reactions have been used to prepare the μ-oxo complexes; one is termed hydrolytic and the other oxidative. The procedures are summarised in Table 1.

(i) Hydrolysis of iron(III) complexes

(a) $Fe(OH)_3$ + ligand

The ligand or ligand salt is added to a suspension of freshly prepared ferric hydroxide in water or ethanol. The complex is usually extracted with and crystallised from an organic solvent.

(b) Fe(ligand)X + base (X = halogen, acetate)

A chloro-iron(III) chelate is dissolved in an organic solvent such as ethanol or chloroform and reacted with aqueous hydroxide or silver oxide. For example, the salen and TPP complexes have been prepared this way[20,32]. If excess KOH is used in the salen case an insoluble, uncharacterised product is obtained.

Triethylamine is a better base for the preparation[35] of bidentate Schiff-base complexes $[Fe(sal\text{-}NR)_2]_2O$. Traces of water are required for the reaction to proceed and there is usually sufficient present in commercial solvents. Sodium carbonate is a good base for R = alkyl. Excess base can again give insoluble polymeric products as found in the tetradentate Schiff-base series.

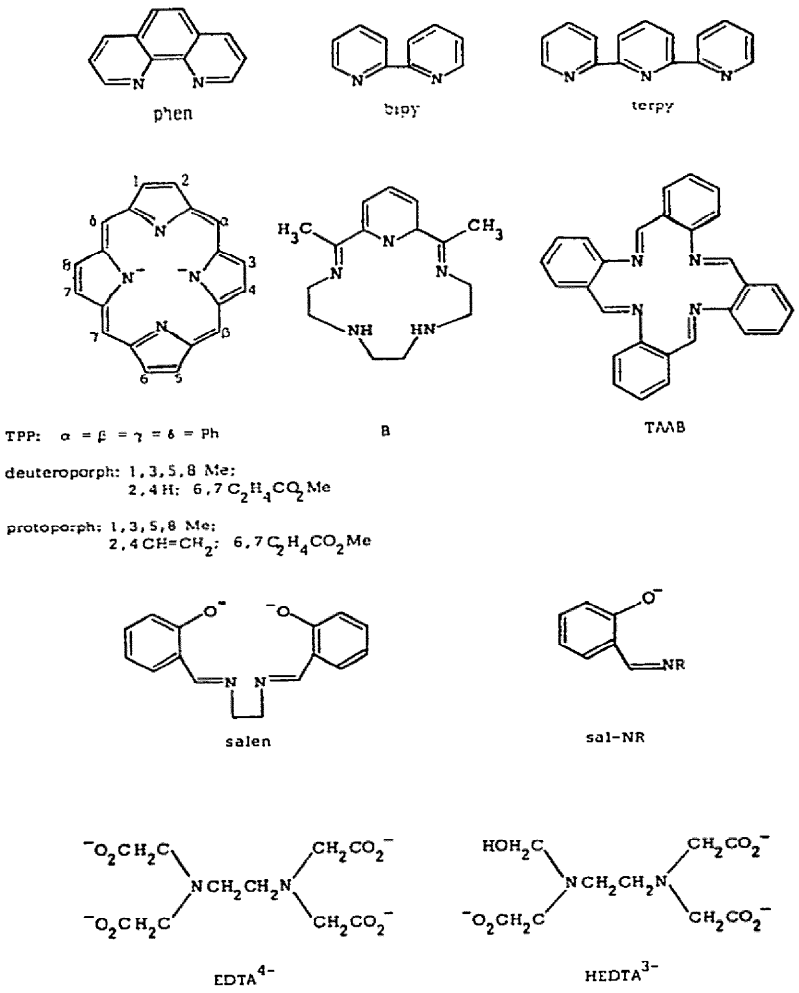

Fig.1. Structures of ligands and their abbreviations.

When [Fe(ligand)acetate] is used as starting material, water only is required for hydrolysis. Salen and porphyrin complexes may be prepared this way[31,40].

Oxo-bridged porphyrin complexes can also be prepared by Al_2O_3 chromatography of the corresponding Fe(porphyrin)X complex (X = Cl, acetate)[31].

(c) Iron(III) salt + ligand

$[(Fe\ phen_2)_2O]^{4+}$ and the bipy analogue are prepared by reacting an aqueous solution of an iron(III) salt with a suspension of the ligand in water. Difficulty is encountered in obtaining pure samples[21,25].

In none of these hydrolytic procedures is there any report of the isolation of the possible monomeric intermediate Fe(ligand)OH.

TABLE 1

Preparative procedures for μ oxo-iron complexes

Complex	Preparative method[a]	Comments	Ref.
$(Fe\ salen)_2O$	(*i*)(*a*) $Fe(OH)_3$ + ligand		20
$[(Fe\ HEDTA)_2O]^{2-}$	(*i*)(*a*) $Fe(OH)_3$ + ligand	pH 5	37
$[(Fe\ EDTA)_2O]^{4-}$	(*i*)(*a*) $Fe(OH)_3$ + ligand	pH 9	37
$(Fe\ salen)_2O$	(*i*)(*b*) Fe(ligand)X + base	X = halide, base = KOH or Ag_2O	20
		X = acetate, base = H_2O	40
$(Fe(sal\text{-}NR)_2)_2O$	(*i*)(*b*) Fe(ligand)X + base	X = halide, base = Et_3N or Na_2CO_3, trace H_2O	35
$(Fe\ TPP)_2O$	(*i*)(*b*) Fe(ligand)X + base	X = halide, base = KOH	32
$(Fe\ porphyrin)_2O$	(*i*)(*b*) Fe(ligand)X + base	X = acetate, base = H_2O, ligand = deuteroporphyrin dimethyl ester	31
$(Fe\ porphyrin)_2O$	(*i*)(*b*) Fe(ligand)X chromatography on Al_2O_3	X = Cl, ligand = deuteroporphyrin dimethyl ester and protoporphyrin IX dimethyl ester	31
$[(Fe\ phen_2)_2O]^{4+}$	(*i*)(*c*) Fe^{III} salt + ligand	Aqueous solution. No added base	21, 25
$[(Fe\ bipy_2)_2O]^{4+}$	(*i*)(*c*) Fe^{III} salt + ligand	Aqueous solution. No added base	21
$[(FeB(H_2O))_2O]^{4+}$	(*ii*) Oxidation of Fe^{II} complex	Oxidised with O_2/H_2O	39
$[(Fe\ terpy)_2O]^{4+}$	(*ii*) Oxidation of Fe^{II} complex	Oxidised with PbO_2/H_2SO_4	27
$(Fe\ salen)_2O.py_2$	(*ii*) Oxidation of Fe^{II} complex	Air oxidation in pyridine solution	14, 40
$(Fe\ porphyrin)_2O$	(*ii*) Oxidation of Fe^{II} complex	Autoxidation in solution	30

[a] See text for classification of methods.

(ii) Oxidation of iron(II) complexes

When an aqueous solution of $FeCl_2 4H_2O$ and the macrocyclic ligand B is reacted in the presence of air, the μ-oxo iron(III) complex is formed and precipitated as the perchlorate salt[39].

As soon as air is admitted to a solution of Fe^{II} salen in an organic solvent, such as pyridine, orange/red crystals of the iron(III) complex are obtained[40]. (A previous publication[41] referring to Fe salen is obviously in fact referring to (Fc salen)$_2$O.) The deuteroporphyrin IX dimethyl ester complex can also be synthesised by this method.

The terpyridine complex $[(Fe\ terpy)_2O](NO_3)_4$, is obtained by oxidising aqueous (Fe $terpy_2)^{2+}$ with PbO_2 followed by addition of a nitrate salt. The addition of Cl^- or ClO_4^- salts yields monomeric derivatives[27].

C. MECHANISM OF DIMER FORMATION AND DISSOCIATION

Because of its relevance to an understanding of the formation of the μ-oxo chelate complexes, this section will begin with a short discussion on the nature of the dimeric species formed in aqueous solutions of simple iron(III) salts. This dimer is often termed the "aquo dimer".

(i) Hydrolysis of aqueous iron(III) solutions

Recent studies on the nature of the dimeric species present in dilute aqueous solutions of iron(III) at low pH are discussed here[42]. The main question is whether the dimer exists as the dihydroxo form $[(H_2O)_4Fe(OH)_2Fe(H_2O)_4]^{4+}$ or as the oxo form $[(H_2O)_5Fe{-}O{-}Fe(H_2O)_5]^{4+}$ in solution. It is normally represented as the former, though very early studies by Jander assumed the oxo form[43,44].

Lutz and Wendt[45,46], Sommer and Margerum[47], and Sutin and co-workers[48,49] have recently studied the rate of dissociation of the aquo dimer using stopped-flow techniques. The equilibria between dimer and monomer are described by eqns. (1) and (2), the latter being an acid-dependent pathway.

$$Fe(OH)_2Fe^{4+} \underset{}{\overset{k_a}{\rightleftharpoons}} 2\ FeOH^{2+} \qquad (1)$$

$$Fe(OH)_2Fe^{4+} + H^+ \overset{k_b}{\rightleftharpoons} Fe^{3+} + FeOH^{2+} + H_2O \qquad (2)$$

Both of these steps involve the slow formation of single-hydroxo-bridged dimeric intermediates. The observed rate of dissociation follows a two term law

$$k_{obs} = [k_a + k_b(H^+)]\ [Fe_2(OH)_2{}^{4+}]$$

The ratio k_b/k_a is similar to those found for other known dihydroxo-bridged complexes. This is taken as support for the presence of a diol bridge in the aquo dimer, although as

Wendt[45] points out, the rate studies do not rule out the alternative formation of a μ-oxo bridge by an inner molecular reaction of the type

$$(H_2O)_5Fe(OH)Fe(OH)(H_2O)_4^{4+} \rightleftharpoons (H_2O)_5Fe{-}O{-}Fe(H_2O)_5^{4+} \quad (3)$$

The magnetic moment of aqueous iron(III) solutions decreases on raising the pH and this has been attributed to the formation of a diamagnetic aquo dimer[50]. Schugar et al.[37] have recently shown that the dimer in solution is paramagnetic, μ_{eff} per Fe ~3.7 B.M., a value which they consider to be compatible with a dihydroxo structure. This seems reasonable in view of the much lower μ_{eff} values observed in Fe–O–Fe complexes (discussed later), but there is the possibility that traces of high-polymer hydrolysed species of similar μ_{eff}, may have been present[11]. Evidence against oxo-bridging in the aquo dimer is given by the lack of a characteristic ν(Fe–O–Fe) band in the infrared spectrum. In contrast, aqueous solutions of the HEDTA–iron(III) dimer do show this band, and its presence after D_2O exchange confirms the existence of $[(HEDTA)Fe{-}O{-}Fe(HEDTA)]^{4-}$ in solution[37].

The bulk of the available evidence appears to favour a dihydroxo bridge in the aquo dimer.

(ii) Hydrolysis of iron(III) chelates

A large number of the μ-oxo complexes may be prepared by hydrolysis of monomeric $Fe^{III}LX$ species in non-aqueous solvents. The reaction pathway presumably involves initial hydrolysis followed by condensation to the dimer. It can be simply represented

$$FeLX + OH^- \rightleftharpoons FeLOH + X^- \quad (4)$$

$$2\ FeLOH \rightleftharpoons (FeL)_2O + H_2O \quad (5)$$

(The reverse reaction $(FeL)_2O + 2\ X^- + H_2O \rightarrow 2\ FeLX + 2\ OH^-$ normally proceeds smoothly and can be used as a synthetic method for the monomer (X = halide, SCN^-, acetate, etc.).)

The hydroxo intermediate FeLOH has not been detected or isolated. There have, however, been no careful mechanistic studies on these nonaqueous methods.

Caughey and co-workers[31] have put forward a number of possible mechanisms involving monomeric or dimeric intermediates. They refer specifically to L = porphyrin but can be considered as general. He modifies the above scheme to incorporate initial ionisation of FeLX, since it is known that X can be exchanged with other ligands Y (e.g. X = acetate, Y = halide)

$$FeLX \rightleftharpoons FeL^+ + X^- \quad (6)$$

$$FeL^+ + H_2O \rightleftharpoons FeLOH + H^+ \quad (7)$$

$$FeLOH + FeL^+ \rightleftharpoons LFeOFeL + H^+ \quad (8)$$

He suggests the possibility of a dihydroxo intermediate in eqn. (5)

$$2\ FeLOH \rightleftharpoons LFe(OH)_2FeL \rightleftharpoons LFe{-}O{-}FeL + H_2O \quad (9)$$

or a mixed-bridge alternative

$$FeLOH + FeLX \rightleftharpoons LFe\begin{matrix}OH\\X\end{matrix}FeL \rightleftharpoons LFe{-}O{-}FeL + HX \qquad (10)$$

Equation (10) would explain the ready conversion of dimer to FeLX in the presence of X^- salts.

Mechanistic studies have been made on aqueous solutions of $(FeEDTA)_2O^{4-}$ and good evidence is presented for the existence in solution of the monomer $Fe(EDTA)OH^{2-}$. Wilkins and Yelin[51], using temperature-jump and stopped-flow methods have investigated the rapid monomer–dimer equilibria shown in eqns. (11)–(13) (L = $EDTA^{4-}$, pH = 6–9)

$$FeL(H_2O)^- \rightleftharpoons FeLOH^{2-} + H^+ \qquad (11)$$

$$2\,FeL(H_2O)^- \rightleftharpoons (FeL)_2O^{4-} + 2\,H^+ + H_2O \qquad (12)$$

$$2\,FeLOH^{2-} \rightleftharpoons (FeL)_2O^{4-} + H_2O \qquad (13)$$

At pH 9 the predominant equilibrium is (13) with only a small contribution from the acid-dependent equilibrium (12). The dimer dissociation is described by a two-term rate law similar to that for the aquo dimer given in section C(i). The dissociation is strongly acid-catalysed in the EDTA dimer, but not in the aquo dimer, the rate constant k_b for the latter being a factor of ca. 10^8 smaller. The difference in rates is considered to reflect a more easily protonated and disrupted bridge in the Fe–O–Fe dimer than in the less basic $Fe(OH)_2Fe$ case. The EDTA and aquo dimers show similar uncatalysed dissociation rates (13) and it has been suggested[52] that in the EDTA system this is due to the transient formation of a dihydroxo-bridged intermediate. Rate studies on the formation of the HEDTA dimer at pH 6.7 showed [51] that it was formed more easily from a combination of $FeL(H_2O)^-$ and $FeLOH^{2-}$ than from two $FeLOH^{2-}$ monomers, and reasons such as charge repulsions and Fe–O bond strength differences were put forward to explain this. Electrochemical measurements on the EDTA system showed good agreement with the kinetic studies[52]. A recent stopped-flow study on the monomer–dimer equilibrium of a water-soluble *p*-sulphonated tetraphenylporphin complex, 2 FeTPPS $\rightleftharpoons$ $(FeTPPS)_2O$, also showed rate behaviour similar to that of the EDTA system[53].

The rate constants for the dimeric iron(III) chelates are given in Table 2 and are compared with those of the aquo dimer. As discussed above, the large differences between k_b for the chelate and the aquo dimer (and other dihydroxo-bridged dimers) is considered to be indicative of μ-oxo bridging in the chelate complexes. The data for the porphyrin system fall in an intermediate range. To date the only dimeric iron(III) chelate complex thought to have a dihydroxo bridge is $[Fe\ picolinate_2OH]_2$; magnetic studies[54] on solid samples show a μ_{eff} value larger than those of other μ-oxo complexes and the aquo-dimer but reduced from the spin-free value.

TABLE 2

Kinetic data for decomposition[a] of μ-oxo iron(III) dimers at 25°C

Ligand	k_a (sec^{-1})	k_b ($M^{-1}.sec^{-1}$)	$\frac{k_b}{k_a}$ (M^{-1})	Ref.
EDTA[b]	1.2	5.0×10^8	4.2×10^8	51
HEDTA[b]	4.0	3.0×10^6	7.5×10^5	51
CyDTA[b]	9.0	$\sim 10^{10}$	$\sim 10^9$	51
TPPS[c]	41.0	840	20.5	53
H_2O[d]	0.42	3.33	7.9	45–49

[a] Acid-independent:

$$LFe{-}O{-}Fe{-}L + H_2O \overset{k_a}{\rightleftharpoons} 2\ FeLOH$$

$$(H_2O)_4Fe(OH)_2Fe(H_2O)_4 + 2\ H_2O \rightleftharpoons 2\ (H_2O)_5FeOH$$

Acid-dependent:

$$LFe{-}O{-}FeL + H^+ + H_2O \overset{k_b}{\rightleftharpoons} FeL(H_2O) + FeLOH$$

$$(H_2O)_4Fe(OH)_2Fe(H_2O)_4 + H^+ + 2\ H_2O \rightleftharpoons Fe(H_2O)_6 + (H_2O)_5FeOH$$

$$k_{dissoc} = (k_a + k_b\,[H^+])[Fe_{dimer}]$$

[b] $\mu = 1.0$ ($NaNO_3$); CyDTA ≡ *trans*-1,2-cyclohexanediaminetetraacetate.

[c] $\mu = 0.1$ ($NaNO_3$); TPPS ≡ tetra(*p*-sulphophenyl)porphin.

[d] $\mu = 3.0$ ($HClO_4/NaClO_4$).

(iii) Oxidation of iron(II) complexes

Traces of moist air will quickly oxidise dark-brown solutions of Fe salen to the red/orange μ-oxo iron(III) compound. Similar oxidations occur for Fe^{II}–porphyrin complexes; kinetic and synthetic studies have been carried out in pyridine and other non-aqueous solvents by Caughey and co-workers[30,31,55].

The overall stoichiometry of the reaction corresponds to the oxidation of four iron(II) porphyrin groups by one oxygen molecule. The mechanism[30,31,55] involves initial ionisation of one pyridine molecule followed by reaction of O_2 with two of the five-coordinate iron(II) moieties

$$py_2FeL \rightarrow pyFeL + py \quad (14)$$

$$2\ pyFeL + O_2 \rightarrow pyLFeO_2FeLpy \quad (15)$$

Some support for the O_2-bridged dimeric intermediate is given by the ability to isolate solid oxygen-adducts[30]. Two alternative pathways have been proposed for further reaction of the O_2-bridged dimer, one[55] involving the presence of water and production of hydrogen peroxide

$$pyLFeO_2FeLpy + 2\,H_2O^* \rightarrow 2\,FeLO^*H + H_2O_2 + 2\,py \quad (16)$$

$$2\,py_2FeL + H_2O_2 \rightarrow 2\,FeLOH + 4\,py \quad (17)$$

(the asterisk * signifies O in H_2O) the other[30] requiring no water

$$pyLFeO_2FeLpy \rightarrow 2\,pyLFeO \quad (18)$$

$$2\,pyLFeO + 2\,pyFeL \rightarrow 2\,pyLFeOFeLpy \quad (19)$$

The μ-oxo dimer shown in eqn. (19) is the final product and has been isolated and characterised. Its formation from the fast reaction (16) most probably involves a doubly bridged intermediate

$$FeLOH + FeLO^*H \rightarrow LFe\begin{matrix}O^*H\\OH\end{matrix}FeL \longrightarrow \quad (20)$$

$$\tfrac{1}{2}(FeL)_2O + \tfrac{1}{2}(FeL)_2O^* + \tfrac{1}{2}H_2O + \tfrac{1}{2}H_2O^*$$

Equation (20) explains the incorporation of oxygen from water observed in autoxidation reactions of py_2FeL with ^{18}O-enriched water. A doubly bridged intermediate would also explain the ability of the bridging oxygen atom in pyLFeOFeLpy to exchange with water[31].

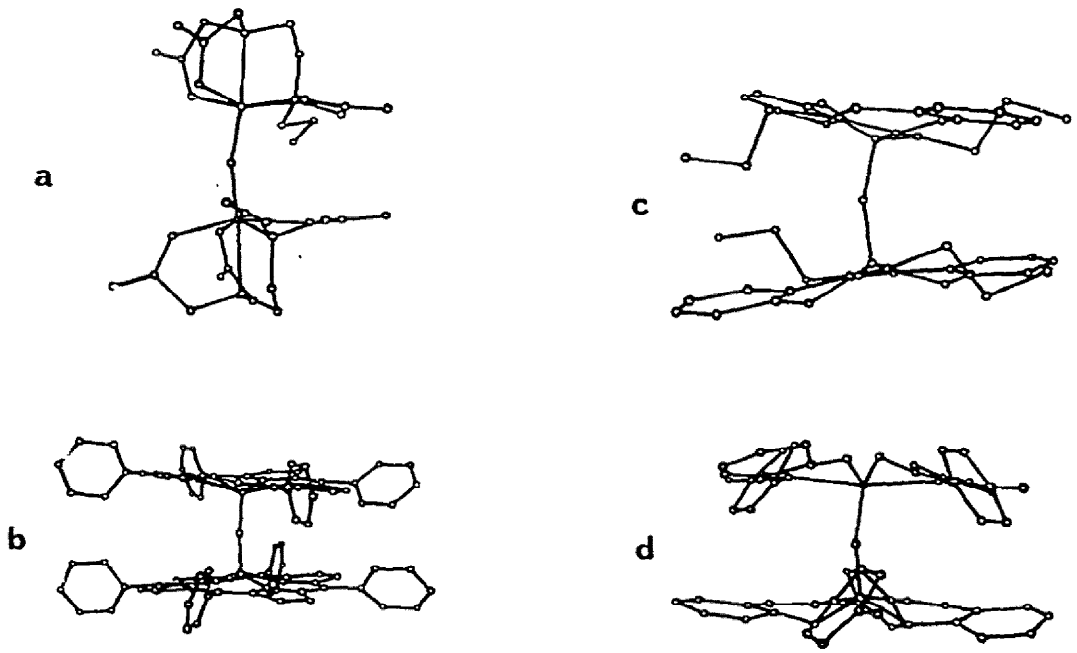

Fig.2. X-ray structures of μ-oxo iron(III) complexes shown with the Fe–O–Fe plane in the plane of paper. (a) $enH_2[(FeHEDTA)_2O].6H_2O$; (b) $(FeTPP)_2O$; (c) $(Fe(sal\text{-}N\text{-}n\text{-}C_3H_7)_2)_2O$; (d) $(Fe(sal\text{-}N\text{-}p\text{-}ClC_6H_4)_2)_2O$.

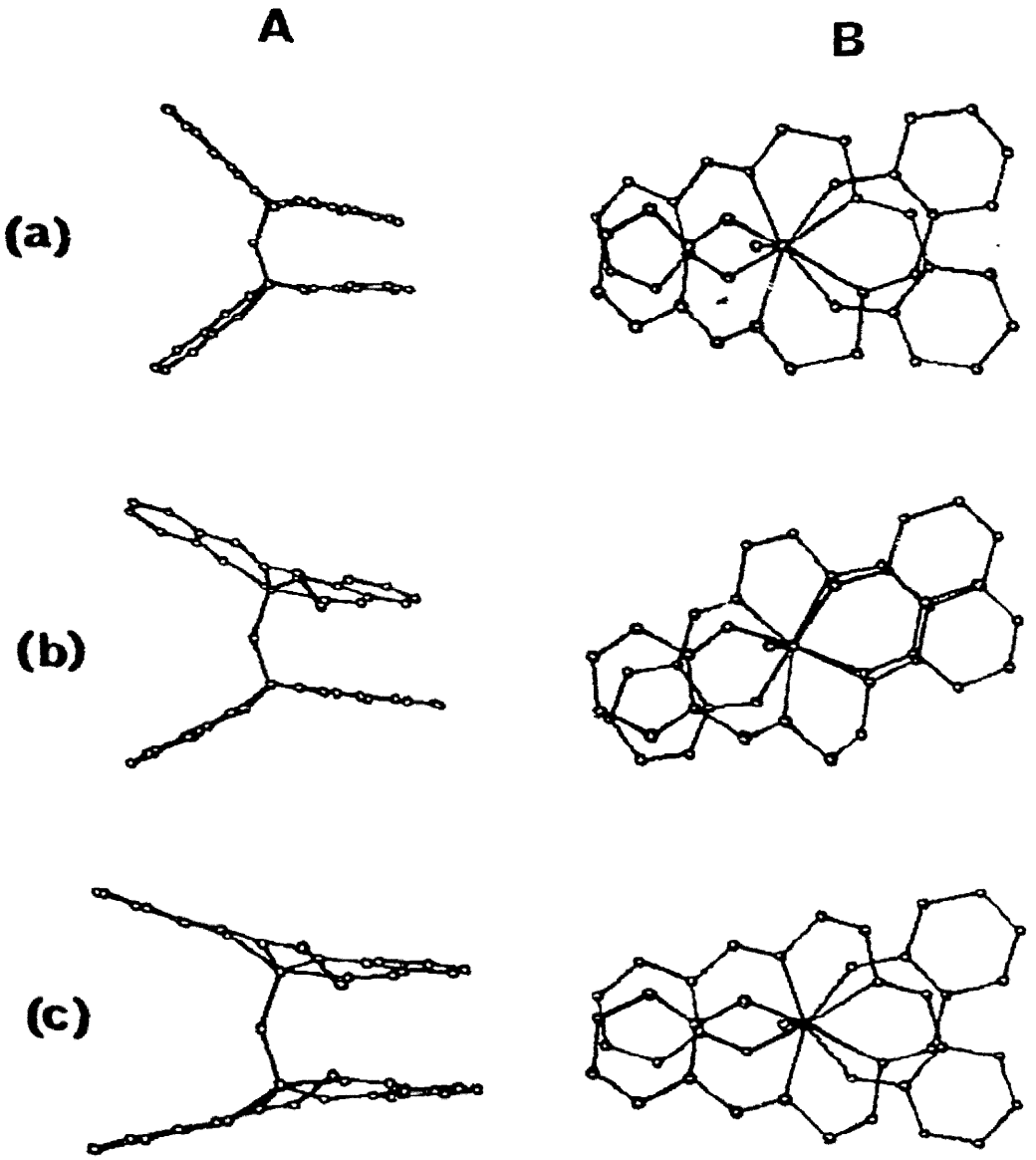

Fig.3. X-ray structures of μ-oxo iron(III)-salen complexes. (A) With Fe–O–Fe plane in plane of paper, and (B) looking down Fe–Fe direction. (a) (Fe salen)$_2$O.py$_2$; (b) (Fe salen)$_2$O.CH_2Cl_2; (c) (Fe salen)$_2$O.

D. X-RAY STRUCTURAL DATA

The detailed molecular structures of seven μ-oxo iron(III) complexes are known. They are shown in Figs. 2 and 3(A) in a projection such that the Fe–O–Fe plane lies in the plane of the paper. Certain gross features are of interest. The common coordination number

TABLE 3

Fe–O–Fe geometry

Numbers in parentheses are estimated standard deviations in the least significant digits. Approximate errors are given by multiplying this figure by ± 3.

	C.N. of Fe	∠FeOFe (°)	*l*(Fe–O) (Å)	*l*(Fe–Fe) (Å)	Ref.
$enH_2[(Fe\ HEDTA)_2O]6H_2O$	6	165(1)	1.79(1)	3.56(1)	62
$[(FeB(H_2O))_2O](ClO_4)_4$	7	178	1.8	3.6	56
$(FeTPP)_2O$	5	174.5(1)	1.763(1)	3.53(1)	61
$(Fe\ salen)_2O$[a]	5	144(1)	1.77(1)	3.39(1)	57
$(Fe\ salen)_2O.py_2$	5	139(1)	1.82(2)	3.36(1)	58
$(Fe\ salen)_2O.CH_2Cl_2$	5	142(1)	1.79(1)	3.40(1)	59, 60
$(Fe(sal\text{-}N\text{-}n\text{-}C_3H_7)_2)_2O$	5	164(2)	1.77(2)	3.51(1)	63
$(Fe(sal\text{-}N\text{-}p\text{-}ClC_6H_4)_2)_2O$[b]	5	175(1)	1.76(1)	3.53(1)	64

[a] Prepared by recrystallising [Fe salen(acetate)] from methanol.
[b] Isostructural with p-BrC_6H_4 derivative.

around the iron is five but there are some examples of six and seven. The Fe–O–Fe angle is non-linear in all cases (except perhaps for $[(FeB(H_2O))_2O]^{4+}$, not shown[56]). In the three salen structures the ligands on each iron are arranged in a non-parallel manner[57–60]. $(FeTPP)_2O$ has the "paddle-wheel" structure[61].

Pertinent angles and distances are given in Table 3. The bridging Fe–O distance is ca. 1.8Å in all cases, which is shorter than the other iron–ligand Fe–O bond length (ca. 1.92Å). This bond shortening is generally considered indicative of some degree of π-bonding along the Fe–O–Fe bridge. Similar effects have been observed in other M–O–M systems (including Al–O–Al)[65–71].

The Fe–O–Fe bridging angle is of particular interest. In view of the linearity of the bridge in other M–O–M complexes (Table 4), it was initially surprising to find the Fe–O–Fe angle deviating so much from 180°. Linearity in M–O–M systems has been ascribed to strong π-bonding and deviations from linearity to a lesser amount of π-bonding. Conversely, σ-type oxygen, as in water, can be considered the normal condition with deviation from the tetrahedral angle towards linearity due to non-bonding (steric) interactions and π-bonding.

It is very difficult to say with certainty what controls the Fe–O–Fe angle in a particular complex, since a variety of effects such as ligand repulsions, electronic and crystal-packing could all play a part. One distinct feature which emerges from Table 3 is the lower angle in the $(Fe\ salen)_2O$ systems, ca. 140°, compared with the angle of 165–175° in all the other complexes studied. Again it is not easy to explain this, though a number of points are perhaps relevant. Compared to the $[Fe(sal\text{-}NR)_2]_2O$ complexes, where the bidentate ligands have *trans*-oxygen and *trans*-nitrogen arrangements[35,63,64], the salen ligand constrains its donor atoms around Fe to be mutually *cis*. This may lead to strain. The non-planarity of

TABLE 4

M–O–M geometry in some oxo-bridged dimers

	C.N. of M	∠M–O–M (°)	*l*(M–O) (Å)	*l*(M–M) (Å)	Ref.
$[(Cr(NH_3)_5)_2O]Cl_4.H_2O$	6	180	1.82	3.64	65–67
$(MnPc)_2O.py_2$	6	178	1.71	3.42	68
$K_4[(ReCl_5)_2O].H_2O$	6	180	1.86	3.72	69
$K_4[(RuCl_5)_2O].H_2O$	6	180	1.80	3.60	70
$(Al(2\text{-Me-oxine})_2)_2O$	5	180	1.68	3.34	71

the iron–salen moieties in (Fe salen)$_2$O.py$_2$ and (Fe salen)$_2$O.CH$_2$Cl$_2$ compared to (Fe salen)$_2$O would suggest that the adducts are highly strained[57–60]. The Fe–O–Fe angle in these salen dimers is not influenced by the adduct molecules in the lattice. In Fig.3(B) the salen dimers are shown looking down the Fe–Fe direction. Though the ethylene bridge is mutually *trans* in the three molecules, the salen groups on each side of the dimer are eclipsed to some degree in all cases. The pyridinate and unsolvated complex show very similar configurations in this projection. This eclipsed arrangement will maximise intramolecular ligand–ligand repulsions. These observations would suggest that intramolecular repulsions and intermolecular packing effects play minor roles in determining the angle.

The Fe–O–Fe angle in (FeTPP)$_2$O is close to 180° since there is a limit to the amount of interaction that can occur between the porphyrin rings[61]. The increase in the angle of the *N*-*p*-chlorophenylsalicylaldiminate complex compared to the *N*-*n*-propyl analogue probably reflects the more bulky substituent on the nitrogen atom in the *N*-aryl case. Gerloch et al. have suggested that the general non-linearity derives from the strength of the Fe–O (bridge) bond[58]. Jezowska-Trzebiatowska[72] considers that it arises for electronic reasons peculiar to iron(III) (see Section K).

The pyridine molecules in (Fe salen)$_2$O.py$_2$ are not bonded to the iron atoms[58]. This contrasts[68] with the case of (Mn phthalocyanine)$_2$O.py$_2$ and is an indication of the stability of five-coordinate structures for high-spin iron(III). In general, the coordination around the iron atoms in these compounds is quite normal for high-spin iron(III); the iron atom is characteristically displaced from the best-plane of donor atoms towards the bridging oxygen atom, viz. 0.5 Å in (FeTPP)$_2$O and 0.56 Å in (Fe salen)$_2$O.py$_2$.

E. INFRARED SPECTRA

The infrared mode commonly used[21,73] to characterise the oxo bridge in iron(III) and other μ-oxo complexes is the antisymmetric stretch ν_{as}(Fe–O–Fe). This appears as a broad, strong band at ca. 820–840 cm^{-1} and in some cases a shoulder is observed at ca. 860 cm^{-1}. In the Schiff-base complexes the band is generally obscured by other ligand bands[20,35]. It is noteworthy that the ν_{as}(Fe–O–Fe) band is observed[21] in the phen and bipy complexes which have previously been formulated[15,74] in the diol form, $[(L_2Fe(OH)_2FeL_2)]^{4+}$.

F. MAGNETIC PROPERTIES

The μ-oxo iron(III) complexes are characterised by low magnetic moment values of ca. 1.9 B.M. per Fe atom. Though these values are reminiscent of those observed in low-spin iron(III) complexes, the temperature dependence of the susceptibility shows th it they cannot belong to this class of compound. The susceptibility drops toward zero as the temperature approaches zero.

As early as 1942 Klemm and Raddatz suggested that the reduced moment in (Fe salen)$_2$O was possibly due to magnetic interactions between iron atoms[16]. Later Mulay and Selwood[50] explained the reduced moments in aqueous iron(III) solutions as being due to the formation of a diamagnetic binuclear species $[Fe(H_2O)_4OH]_2^{4+}$.

Lewis and co-workers subsequently gave a quantitative analysis of the magnetic behaviour using what they somewhat misleadingly termed the "dipolar-coupling" approach[18–20].

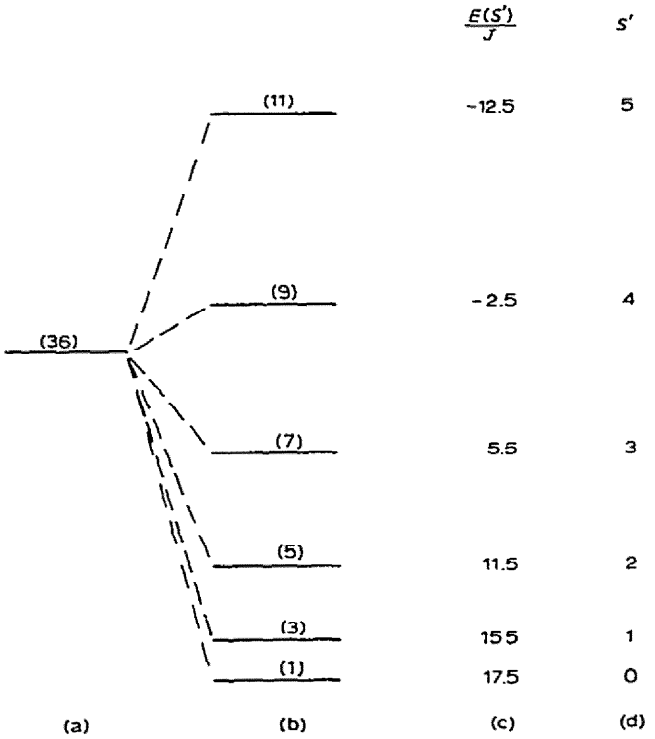

Fig.4. Energy level scheme for a pair of interacting Fe^{3+} ions. (a) Total spin degeneracy of ground state; (b) effect of spin–spin interaction of the form $-2J\bar{S}_i\bar{S}_j$; (c) energy of spin states $E(S')/J$; (d) values of S'.

(i) Theory

The theory, due to Heisenberg[75], Dirac[76] and van Vleck[77] (HDVV), assumes an isotropic exchange interaction between the spins on each iron atom within a binuclear molecule. The appropriate Hamiltonian is $-2\Sigma J_{ij}S_iS_j$, where J_{ij} is the isotropic exchange integral between the ith and jth atoms of spin S_i and S_j. J is negative in the case of antiferromagnetic exchange. For high-spin iron(III), where $S_i = S_j = \frac{5}{2}$ ($^6A_1$ term) a set of spin-states, $S' = 5$, 4, 3, 2, 1, 0 exist with energies $-30J$, $-20J$, $-12J$, $-6J$, $-2J$ and 0, respectively. The energy level diagram is shown in Fig.4. The susceptibility expression derived from the Zeeman splitting of these levels is

$$\chi_{Fe} = \frac{N\beta^2g^2}{kT}\,\frac{\{\exp(2J/kT)+5\exp(6J/kT)+14\exp(12J/kT)+30\exp(20J/kT)+55\exp(30J/kT)\}}{[1+3\exp(2J/kT)+5\exp(6J/kT)+7\exp(12J/kT)+9\exp(20J/kT)+11\exp(30J/kT)]}+N\alpha$$

As the temperature is decreased, the higher S' states are thermally depopulated, until at very low temperatures only the diamagnetic ground state is populated. In classical terms the spins ("dipoles") become aligned antiparallel and the magnetic moment approaches zero.

(ii) Comparison of experimental data with theory

Lewis et al. found that the experimental susceptibilities of the (Fe salen)$_2$O and [(Fe·phen$_2$)$_2$O]$^{4+}$ systems fitted the calculated $S = \frac{5}{2}$ expression extremely well and values of $J = -100$ cm^{-1}, $g = 2.0$ and $N\alpha = 0$ were obtained[19-21]. The magnitude of J was independent of the nature of various substituents on the salen ligand[20]; similar results were found for the complexes [Fe(sal-NR)$_2$]$_2$O, where the substituent R on the nitrogen atom was varied quite widely[78]. In fact, for all of the Schiff-base, diimine and HEDTA oxo-bridged complexes studied so far, the J values are virtually identical, i.e. -90 ($\pm$10) cm^{-1} (Table 5). The magnitude of the exchange interaction therefore appears to be chiefly a property of the Fe–O–Fe bridge and independent of the nature of the ligand group bound to the iron atoms.One exception to this general observation is the recent work[80] on (Fe protoporphyrin IX)$_2$O, which shows a lower μ_{eff} value, 1.55 B.M., and concomitant higher J value, -132 cm^{-1}. (FeTPP)$_2$O, on the other hand, appears to show[53] a J value similar to that of all the other complexes. Early samples showed variable μ_{eff} values[32,33] because the porphyrin complexes present difficulties in obtaining samples free from paramagnetic impurities[32,33,80], a problem met to a lesser degree in a number of the other μ-oxo systems[21,25]. Susceptibility measurements on a number of the complexes down to 4.2°K show an increase at very low temperatures[28,79]. This increase may be due to traces of monomeric impurities, or to inter-dimer interactions as observed recently in other polynuclear compounds[8]. Mössbauer measurements at 4°K do not favour the latter possibility[81].

TABLE 5

Magnetic properties of representative μ-oxo iron(III) complexes

Compound	μ_{eff} at 295°K (B.M.)	$-J(cm^{-1})^a$	Ref.
(Fe salen)$_2$O	1.87	95	19, 20, 27
(Fe(sal-NR)$_2$)$_2$O	1.82–1.94	90–100	78
[(Fe phen$_2$)$_2$O]$^{4+}$	1.74–1.83	95–105	21, 28
[(Fe bipy$_2$)$_2$O]$^{4+}$	1.86	105	21, 28
[(Fe terpy)$_2$O](NO$_3$)$_4$.H$_2$O	1.83	105	28
enH$_2$[(FeHEDTA)$_2$O]6H$_2$O	1.92	95	54, 79
Na$_4$[(FeEDTA)$_2$O]12H$_2$O	1.90	99	79
[(FeB(H$_2$O))$_2$O](ClO$_4$)$_4$	1.94	100	28
(FeTPP)$_2$O	1.86	(100)^b	53
	1.15		32
	1.74		33
(Fe protoporphyrin)$_2$O	1.55	131	80

^{a} $g = 2.0$, $N\alpha$ (T.I.P.) = 0 c.g.s.
^{b} Not fitted to theory.

(iii) Spin-state problem

Monomeric iron(III) complexes can have spin states of $\frac{5}{2}$, $\frac{3}{2}$ and $\frac{1}{2}$ depending on the strength of the ligand field. In antiferromagnetically coupled iron(III) pairs, the energy level diagrams for $(\frac{3}{2}, \frac{3}{2})$ and $(\frac{1}{2}, \frac{1}{2})$ simply correspond to removal, or non-population, of the $S' = 5, 4$ and $S' = 5, 4, 3, 2$ levels, respectively, shown in Fig.4 (assuming absence of orbital angular momentum contribution). Susceptibility measurements on the present complexes have generally been made in the region 300–4°K. For J values of ca. $-100\ cm^{-1}$, the higher S' levels are not significantly populated at 300°K and the susceptibility measurements do not therefore distinguish between the $\frac{5}{2}$ and $\frac{3}{2}$ spin states. Contrary to the recent comments of Cotton and Wilkinson[82], the measurements do eliminate the $S = \frac{1}{2}$ possibility. Other physical measurements, discussed later, show unequivocally that the spin state is $\frac{5}{2}$ in all cases. In order to populate the $S' = 4$ and 5 levels, i.e. completely uncouple the five electrons on each iron, susceptibility measurements to very high temperatures would be required. These, of course, would be limited by the thermal stability of the particular compound.

(iv) Exchange mechanism

The Fe–Fe distances, shown in Table 3, are in the range 3.4–3.6Å. The contribution of direct metal–metal orbital overlap to the exchange mechanism is considered to be small for such separations. Exchange must occur via overlap of the metal d orbitals with the bridging oxygen orbitals, i.e. a superexchange pathway. Martin[7] and Ginsberg[8] have recent-

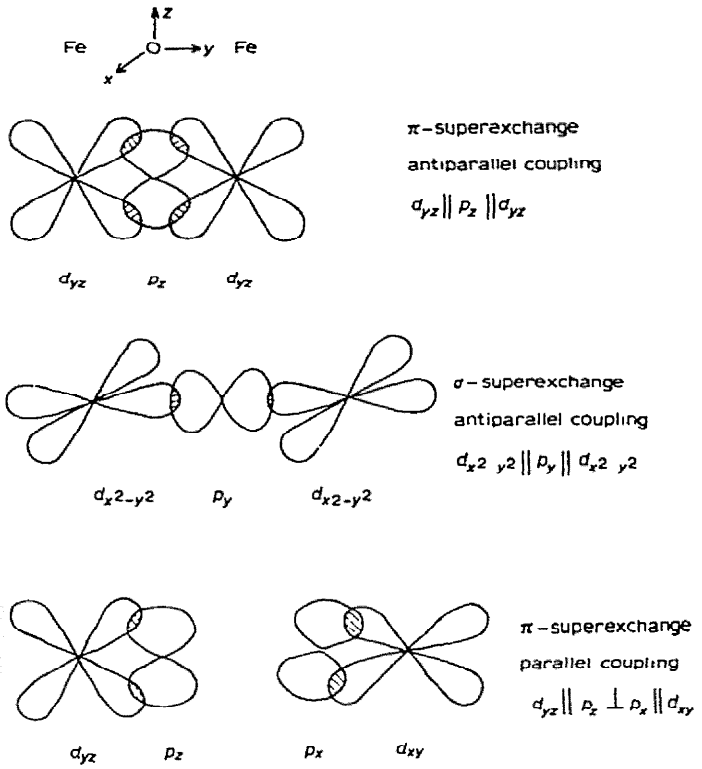

Fig.5. Some examples of superexchange pathways in $(Fe-O-Fe)^{4+}$ bridge.

ly discussed the superexchange theories of Anderson[83] and Goodenough[84] in some detail. In the case of 180° or linear superexchange for d^5-d^5 systems, antiferromagnetic and ferromagnetic pathways both occur, but the direct overlap between e_g(Fe) and p_y(O) orbitals dominates and leads to overall antiferromagnetism (Fig.5). Anti-parallel coupling is also predicted in 90° d^5-d^5 superexchange. The antiferromagnetism of the present complexes is therefore in agreement with theoretical predictions.

The higher value of J in the $(Fe\ porphyrin)_2O$ complexes[80] can be rationalised in terms of greater π-overlap arising from a more linear Fe–O–Fe bridge. Within the other series of compounds, it is perhaps surprising that the J values for the $(Fe\ salen)_2O$ complexes are the same as all the others, even though the Fe–O–Fe angle is smaller by about 15°. One possible explanation for this is that the changes in superexchange contributions from antiferromagnetic and ferromagnetic pathways, which occur on changing the M–O–M angle, accidentally cancel out.

(v) Single-crystal susceptibility studies

The HDVV model, used successfully to describe the temperature variation of the average

susceptibility of powdered samples, assumes *(i)* isotropic exchange; *(ii)* a formal spin state for each iron atom; and *(iii)* a g value close to the free-electron value of 2.0. Assumption *(iii)* is reasonable in the case of high-spin iron(III), which has an orbitally non-degenerate $^6A_1$ ground term. Anisotropy in such systems would be expected to be negligible unless large zero-field effects are operative due to symmetry effects, as is observed in some monomeric porphyrin iron(III) derivatives[85]. In order to test assumptions *(i)* to *(iii)* more fully, measurement of the anisotropy in the susceptibility and g tensors are required. To date there have been very few single-crystal ESR (discussed below) or susceptibility studies on these, or any other, polynuclear species.

Mabbs and co-workers[59] have measured the magnetic anisotropy of (Fe salen)$_2$O.CH$_2$Cl$_2$ over the temperature range 300–80°K. The crystalline anisotropies, $\Delta\chi/\chi$, were very small, ranging from 3% at 300°K to 1% at 80°K. No allowances could be made for diamagnetic or shape anisotropies which are significant for A ground terms. The principal molecular susceptibilities, K_i, were calculated relative to a set of molecular axes which lay along the Fe–Fe (K_1) direction and its perpendicular bisector (K_2, K_3). This set of molecular axes was presumably chosen for convenience, because in monoclinic crystals there need be no simple relationship between molecular directions and molecular susceptibility directions[86]. With these sources of error in mind, the K_i values were found to be nearly isotropic ($K_1 < K_2 < K_3$). The results therefore show that isotropic exchange between $S = \frac{5}{2}$ iron(III) atoms and $g = 2.0$ are reasonable assumptions for this system. It is noteworthy that a crystalline anisotropy of 40% was observed[87] for the high-spin five-coordinate monomer Fe salen Cl. There has been no subsequent discussion on this measurement but it presumably arises from zero-field splitting effects which, interestingly, are much reduced in formation of the Fe–O–Fe bridge. Negligible zero-field splitting was also observed for (Fe deuteroporph)$_2$O using far infrared methods[31].

Anisotropy measurements on enH$_2$ [(FeHEDTA)$_2$O] 6H$_2$O are currently in progress[88]. An unusual feature to emerge so far is the very large change in setting position of the crystal with decreasing temperature when suspended with the a axis vertically. Since a principal crystal susceptibility should set along (or at 90° to) the field direction in this orientation, the observation implies that the susceptibility directions are changing with temperature. Variable temperature X-ray measurements are being made to see if structural changes are occurring which might give this effect.

G. ESR SPECTRA

The only reported ESR study is the preliminary report by Okamura and Hoffman[89] on single crystals of enH$_2$ [(FeHEDTA)$_2$O] 6H$_2$O. At X-band a complex signal of line width ca. 150 gauss was observed, and assigned to transitions arising from the spin state $S' = 2$ (see Fig.4). The intensity of the band decreased with decreasing temperature in much the same manner as the susceptibility, and a J value of -95 cm^{-1} was obtained by comparison with the theoretical expression for intensity. At Q-band, with the applied field along the b axis of the monoclinic crystal, a simple 4-line spectrum centred at $g_{\text{eff}} = 2$ was observed,

and again assigned to $S' = 2$ transitions. A number of unassigned weaker lines were observed at low field. The g value is consistent with that employed in the susceptibility calculations. An approximate value of the zero-field splitting parameter D of magnitude 0.15 cm^{-1} was obtained within the $S' = 2$ state.

Attempts to obtain ESR spectra on single crystals of (Fe salen)$_2$O.CH_2Cl_2 failed at Q-band[58]. It is not clear why no spectrum is obtained; the usual reasons are the effects of spin–lattice relaxation, dipolar broadening or zero-field splitting being larger than the microwave quantum. X-band spectra at 77°K of powdered or dilute solutions of [Fe(sal-N-*n*-propyl)$_2$]$_2$O show[90] only a near isotropic line at $g_{eff} \simeq 4.3$. A similar spectrum is observed[90] for the five-coordinate monomer Fe(sal-N-*n*-propyl)$_2$Cl and is characteristic of rhombic $S = \frac{5}{2}$ iron(III) systems with zero-field parameters $D \simeq 0.2$ cm^{-1} and $E/D \simeq \frac{1}{3}$. It is possible, but unlikely, that the spectrum of the oxo complex is due to the presence of monomeric impurities.

Finally, mention was made of the single-crystal ESR spectrum at X-band of [(Fe phen$_2$)$_2$O](NO$_3$)$_4$.2H$_2$O, but nothing has subsequently appeared[25]. There is clearly a need for more detailed ESR studies on these molecules.

H. ELECTRONIC SPECTRA

In general, electronic spectral measurements on iron(III) complexes are not the most sensitive probe for an understanding of their electronic and molecular structure. The d–d transitions for $S = \frac{5}{2}$ iron(III), which has a $^6A_1$ ground term, are both spin and Laporte forbidden and hence very weak. The spectra, at least of solutions, are generally dominated by strong ligand or metal–ligand charge-transfer bands. Since many of the present complexes possess beautiful orange/red colours it seemed possible that some band(s), characteristic of the binuclear structure or μ-oxo linkage, might be observable.

(i) Solution and reflectance spectra

Broad, unresolved charge-transfer bands above 15,000 cm^{-1} are shown[27] by (Fe phen$_2$)$_2$O^{4+}, (Fe bipy$_2$)$_2$O^{4+}, (Fe terpy)$_2$O^{4+} and (Fe salen)$_2$O. In the spectra of the polyimine systems and [FeB(H$_2$O)]$_2$O^{4+}, however, bands of intensity $\epsilon \simeq 6$ are shown at ca. 10,000 cm^{-1}. Reiff et al.[27] suggested that the enhanced intensity of this supposedly spin-forbidden visible band might arise from a pair mechanism, similar to that operative in some Mn^{II}–fluoride compounds[91].

Schugar et al.[79] observed bands of similar intensity for (FeHEDTA)$_2$O^{2-} and (FeEDTA)$_2$O^{4-} in the region 11,000–24,000 cm^{-1}, and assigned them to transitions from the $^6A_1$ ground state to singly excited quartet states. The intensities were again thought to be possibly due to the effects of pair interactions. Ligand field parameters $10Dq$ = 10,900 cm^{-1}, B = 950 cm^{-1} and C = 2,300 cm^{-1} were deduced, which are close to those for Fe(H$_2$O)$_6^{3+}$.

In contrast to the broad UV absorption shown by most of the μ-oxo complexes, four fairly well resolved intense bands were given by the HEDTA and EDTA dimers. They ap-

peared at positions which corresponded to the sums of individual singly excited transition energies and have been assigned to simultaneous pair electronic excitations (SPE), that is a simultaneous excitation of two ligand-field transitions. Such a mechanism introduces spin-allowedness, and has been detected recently in other systems[91,92]. Since little definitive evidence, apart from the additivity in band position, was presented for the SPE assignments, they should be regarded with some caution at this stage. A well-characterised example of SPE in Fe–O–Fe systems is described below.

(ii) Single-crystal spectra

Schugar et al.[79] found that enH_2 [$(FeHEDTA)_2O$] $6H_2O$ possesses a dichroic rhomboidal face and a non-dichroic rectangular face. The Fe–O–Fe axis lies almost in the plane of the dichroic face and is perpendicular to the non-dichroic face. The dichroism consists of a strong red and weaker orange absorption, which can lie parallel (red) to or perpendicular (orange) to the Fe–O–Fe direction when the polarised light is normal to the rhomboidal face. The 11,000 cm^{-1} ($^4T_1$) band in the visible region is strongly polarised along the Fe–O–Fe direction and its intensity decreases with decreasing temperature. Bands at 18,400 cm^{-1} ($^4T_2$) and 21,000 cm^{-1} ($^4A_1$, ^4E) are also polarised. No detailed explanation of these observations was given.

Dubicki and Schulberg[93] have looked in more detail at the singly excited $^6A_1 \rightarrow (^4A_1, ^4E)$ transition in enH_2 [$(FeHEDTA)_2O$] $6H_2O$ over the temperature range 300–4°K. Unfortunately, the band was not resolvable into any component lines. Although the intensity of the band was in general accord with an exchange-induced mechanism, the detailed temperature dependence gave poor correlation with spectra simulated using an exchange-coupled model which did not allow for spin–orbit coupling effects.

Ferguson and Fielding[94] have recently shown that the absorption spectrum of natural or synthetic yellow sapphires is due to single Fe^{III} ions and pairs of ions $(Fe–O–Fe)^{4+}$; the present discussion is limited to the pair spectra. The visible spectrum is not complicated by the presence of any ligand bands. The band assignments are given in Table 6 and some corresponding energy level diagrams are shown in Fig.6. Transitions to singly and doubly (SPE) excited pair states have been identified with certainty in this more symmetric system. The positions of the singly excited transitions are the same as those in monomeric iron(III). The intensities of the singly excited spin-flip transitions decrease with decreasing temperature. In one such transition, observation of the expected four component pair lines has allowed an estimation of the ground state exchange integral J of ca. -12 cm^{-1}. This value is much reduced from that in the μ-oxo dimers and corresponds to the fourth nearest-neighbour pairs in the sapphire crystal. The doubly excited transitions appear at approximately the sum of the individual singly excited transition energies, as was found in the HEDTA dimer. Their intensities increase with decreasing temperature because transitions from $S' = 4, 5$ are forbidden, whilst those from $S' = 0, 1, 2, 3$ are allowed under the $\Delta S = 0$ selection rule (Fig.6(b)).

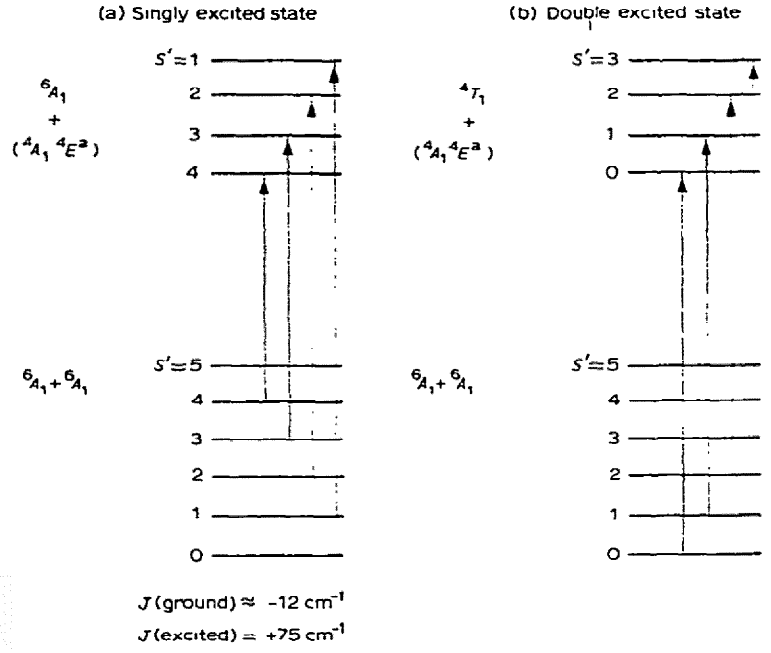

Fig.6. Energy levels of iron(III) pair spectra in yellow sapphire (not drawn to scale).

TABLE 6

$(Fe–O–Fe)^{4+}$ pair spectra in yellow sapphires

Band positions (cm^{-1})	Assignment	Comments
(a) Singly excited states		
9,000	$^6A_1 + {}^6A_1 \rightarrow {}^4T_1 + {}^6A_1$	Spin-flip and orbital change; intensity independent of temperature; highly polarised
13,000	$^6A_1 + {}^6A_1 \rightarrow {}^4T_2{}^a + {}^6A_1$	As above
22,000	$^6A_1 + {}^6A_1 \rightarrow ({}^4A_1, {}^4E^a) + {}^6A_1$	Spin-flip transition; intensity decreases with decreasing temperature; four component pair levels observed (S' = 1, 2, 3, 4)
25,500	$^6A_1 + {}^6A_1 \rightarrow {}^4T_2{}^b + {}^6A_1$	Spin-flip and orbital change
26,500	$^6A_1 + {}^6A_1 \rightarrow {}^4E^b + {}^6A_1$	Spin-flip; intensity decreases with decreasing temperature
(b) Doubly excited states (SPE)		
18,000	$^6A_1 + {}^6A_1 \rightarrow {}^4T_1 + {}^4T_1$	Intensity increases with decreasing temperature
22,000	$^6A_1 + {}^6A_1 \rightarrow {}^4T_1 + {}^4T_2{}^a$	
29,750	$^6A_1 + {}^6A_1 \rightarrow ({}^4A_1, {}^4E^a) + {}^4T_1$	Intensity increases with decreasing temperature

[a] ^4G.
[b] ^4D.

In summary, the positions and intensities of certain bands can in favourable cases be assigned to pair transitions. Unfortunately, for most of the μ-oxo iron(III) complexes, the spectra are not resolved well enough to identify these transitions.

I. ^{1}H NMR CONTACT SHIFT SPECTRA

The ^{1}H NMR spectra of oxo-bridged iron(III) complexes show quite narrow ($\sim$ 50 Hz), well-resolved lines. This is most likely a result of the strong magnetic exchange interactions which give rise to majority population of the diamagnetic $S' = 0$ ground state.

Boyd and Murray[95] developed the theory of the temperature dependence of the Knight shift (contact shift) $\Delta H/H_0$, of a given proton, for a binuclear system, using the HDVV exchange-coupled model discussed in Section F. For an $S = \frac{5}{2}$ system, the dipolar contribution to $\Delta H/H_0$ is generally considered to be very small and was thus set at zero, i.e. the observed shifts were assumed to be contact in origin[96]. The calculated expression for $\Delta H/H_0$ is

$$\frac{\Delta H}{H_0} = \frac{Ahg\beta}{g_n\beta_n kT} \cdot F$$

$$F = \frac{\exp(2J/kT)+5\exp(6J/kT)+14\exp(12J/kT)+30\exp(20J/kT)+55\exp(30J/kT)}{1+3\exp(2J/kT)+5\exp(6J/kT)+7\exp(12J/kT)+9\exp(20J/kT)+11\exp(30J/kT)}$$

The constants have their usual significance. The exponential function is the same as that calculated for χ_{Fe} since the total spin operator $\langle S_z' \rangle$ is used in both situations. As in the susceptibility behaviour, the last two exponential functions from $S' = 4$ and 5 contribute nothing to $\Delta H/H_0$. The hyperfine coupling constant, A, applies to the manifold of S' spin states.

Comparison of experimental and calculated $\Delta H/H_0$ and T values by a fitting procedure thus allowed the determination of J and A for a particular proton. The theory was applied to a series of bidentate Schiff-base dimers, $[Fe(Xsal\text{-}NR)_2]_2O$ (X = H or Me) and good correlation was obtained[95] over the limited range 325–223°K. A typical spectrum is shown in Fig.7; the best-fit J and A values are given in Table 7(a). The variation in J obtained for different protons of a particular complex might be real, but more likely reflects the errors in measurement and fitting. The average J values in $CDCl_3$ solution are approx. 25 cm^{-1} higher than those obtained for solids by susceptibility studies. This was thought to be possibly due to a straightening of the Fe–O–Fe bridge in solution.

Temperature-dependent NMR studies were later made on $(Fe\ porphyrin)_2O$ dimers. Wicholas et al.[97] assumed zero contribution from dipolar effects in some porphyrin dimers but used a different $A_{S'}$ parameter for each paramagnetic S' state. Using a three-parameter procedure they deduced J, A_1 and A_2 values for $(FeTPP)_2O$ and found that A_1 was slightly larger but almost the same as A_2. The J and $A_{S'}$ values were virtually identical with those obtained[98] by a previous two-parameter fit and are given in Table 8. The J value was again higher than that found for the solid.

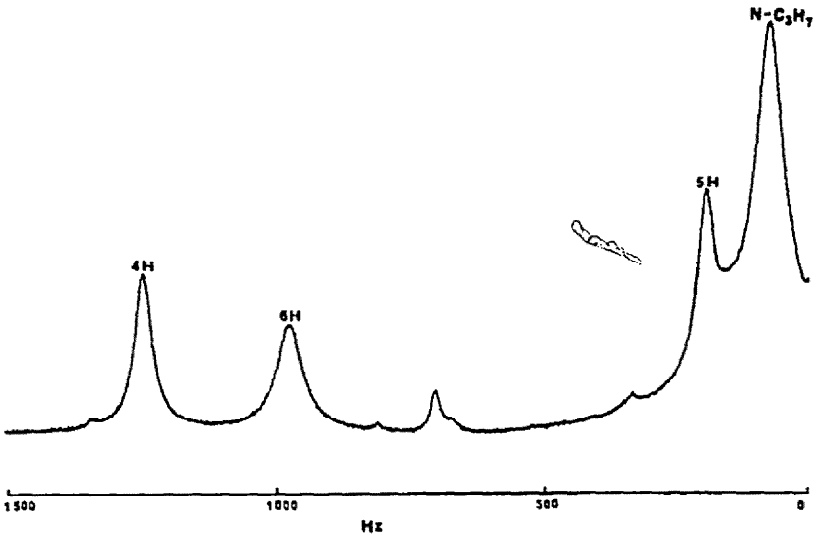

Fig.7. ^{1}H NMR spectrum of (Fe(sal-N-n-C_3H_7)$_2$)$_2$O in $CDCl_3$ solution at room temperature.

TABLE 7

^{1}H NMR data for (Fe(Xsal-NR)$_2$)$_2$O and (Fe(Xsalen))$_2$O complexes in $CDCl_3$ and CD_2Cl_2 solutions

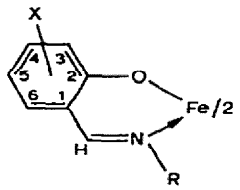

X = H or CH_3
(*a*) R = n-C_3H_7 (ref. 95)
(*b*) R = $-CH_2-$ (ref. 99)

Complex	Ring H								
	4-			5-			6-		
	ΔH	$-J$	$A\times10^{-5}$	ΔH	$-J$	$A\times10^{-5}$	ΔH	$-J$	$A\times10^{-5}$
(*a*)									
X = H	−5.68	116	1.07	+4.41	140	−1.05	−2.88	120	0.577
X = 4-CH_3	(+1.29	112	−0.25)*	+4.59	135	−1.04	−2.84	140	0.686
X = 5-CH_3	−5.58	116	1.05	(−5.14	122	1.032)*	−2.87	145	0.731
(*b*)									
X = H	−5.93			+4.74			−2.97		
X = 3-CH_3	−7.09			+5.02			−3.20		
X = 4-CH_3	(+1.14)*			+4.75			−2.82		
X = 5-C_4H_9	−5.45		1.10(A_1)(−0.29)*				−2.75		
			2.21(A_2)						
			0.44(A_3)						

* Methyl, t-butyl.
ΔH in p.p.m. at room temperature (relative to free ligand position), J in cm^{-1} ($2J$ = singlet–triplet splitting), A in Hz.

TABLE 8

^{1}H NMR data* and J values for (Fe porphyrin)$_2$O complexes in $CDCl_3$ solution

Complex	Pyrrole H			Meso H	Meso-phenyl H
	ΔH (p.p.m.)	$-J$ (cm^{-1})	$A \times 10^{-5}$ (Hz)	ΔH (p.p.m.)	ΔH (p.p.m.)
$(FeTPP)_2O$[a]	−4.64	155	1.29		~0
$(FeTPP)_2O$[b]	−4.64	155	1.28(A_1) 1.22(A_2)		~0
$(FeTPP)_2O$[c]	−5.02				~+0.05
(Fe deut)$_2$O	−4.62			+8.44	
(Fe proto)$_2$O				+8.28	

* Only pyrrole and meso protons listed.
(a) Ref. 98, shifts relative to free ligand.
(b) Ref. 97, shifts relative to free ligand.
(c) Ref. 99, shifts relative to $(ScTPP)_2O$.

In a recent study of salen and porphyrin systems La Mar et al.[99] claim that the use of one A value and zero contribution from dipolar shifts does not allow the calculation of accurate J and A values by the fitting procedures described above[95,98]. They used the assumption that any zero-field splitting (ZFS) in monomeric FeLX species would mean a similar ZFS in the analogous $(FeL)_2O$ complex and hence a dipolar contribution to the total shift. While it is known that Fe salen Cl and Fe porphyrin Cl complexes show quite large D values[85,87], measurements made so far on the related oxo-bridged dimers show[31,58,89] very small or zero D values (see Section F). La Mar et al., in fact, found zero D value in (Fe salen)$_2$O type complexes, i.e. just a contact shift, but from the $\Delta H/H_0$ vs. T behaviour of FeTPPCl, which was non-Curie, they inferred a non-zero value in $(FeTPP)_2O$ with a consequent dipolar contribution to the shift. They compared the χ_{Fe} (solid) and $\Delta H/H_0$ vs. T curves for (Fe salen)$_2$O and found that these curves diverged from a normalised point. This divergence was considered to imply a different $A_{S'}$ value for each S' state and in the case of (Fe salen)$_2$O it was found that $A_1 < A_2$. Approximate values of $A_{S'}$ were deduced and are given in Table 7(b). For equal $A_{S'}$ the curves would be superimposable and the $\Delta H/H_0$ expression given above valid. Comparison of χ_{Fe} and $\Delta H/H_0$ curves for $(FeTPP)_2O$ showed very little divergence but sufficient to suggest $A_1 > A_2$.

From the foregoing discussion it is seen that there are opposing views on the theoretical interpretation of the NMR data, one using a single A value[95,98] to describe the system, the other using a number of $A_{S'}$ values[97,99]. The hyperfine constant is introduced in the contact shift term. A weakly coupled Heisenberg model was assumed in both interpretations and the available evidence shows that these iron(III) dimers belong to this class. The orbital

wave function for the various S' states is the same. Unpaired electrons cannot be assigned to particular orbitals[99]. Thus, the spin density will not be different for different S' states, i.e. there is only one spin polarisation mechanism. This is shown in the theoretical derivation[95] where the hyperfine parameter is associated with the total spin quantum number

$$\Delta H/H_0 = \frac{Ah\langle S'_z\rangle}{2g_n\beta_n}$$

and not with a particular spin state. The use of one A value is therefore correct under these circumstances. McGarvey and Kurland have discussed[96] systems which require more than one A value but these generally involve different orbital states. They also showed that appreciable ZFS in iron(III) monomers had negligible effect on the Fermi contact interaction. The divergence of $\Delta H/H_0$ and χ curves observed by La Mar et al.[99] could be due to experimental errors in the two measurements.

Bearing these various arguments in mind, the A values shown in Tables 7 and 8 are similar in magnitude to those observed[100] for low-spin $^2T_{2g}$ iron(III) complexes, i.e. 10^4-10^5 Hz. The signs of $\Delta H/H_0$ for the ring protons in $[Fe(sal\text{-}NR)_2]_2O$ and $(Fe\ salen)_2O$ are given in Table 7. The alternating sign pattern, together with the change in sign on substituting CH_3 for H, are indicative of a π-spin delocalization mechanism[101]. The sign of $\Delta H/H_0$ for the porphyrin ring protons has been correlated with a predominantly σ-mechanism[97].

NMR spectra of $(Fe\ phen_2)_2O^{4+}$, $(Fe\ bipy_2)_2O^{4+}$ and their substituted derivatives have also been obtained[102,103].

J. MÖSSBAUER EFFECT SPECTRA

Mössbauer effect studies on the oxo-bridged iron(III) complexes were some of the first studies on polynuclear iron systems. Isomer shift and quadrupole splitting parameters have been obtained with zero applied magnetic field by a number of workers, and the results are given in Table 9.

The δ values are all in the region of ca. 0.7 mm.sec^{-1} at 300°K which is indicative of an $S = \frac{5}{2}$ iron(III) state. The Schiff-base, porphyrin and macrocyclic (B) compounds show ΔE values < 1 mm.sec^{-1}, whilst the diimine and polyamino carboxylic acid compounds show ΔE between 1.5–2.0 mm.sec^{-1}. The former value is in the range normally observed for $S = \frac{5}{2}$ iron(III) while the latter are much higher. The significance of these ΔE values must await molecular orbital calculations on bonding effects around the iron atoms.

Buckley et al. have rationalised relaxation and asymmetry effects in the spectra of dimeric iron compounds[104–107]. In general they have shown that asymmetry arises due to spin–spin relaxation between dimers (intermolecular) rather than within the dimer as earlier proposed[108,114a] (intramolecular). In the case of $(Fe\ salen)_2O$ a symmetric quadrupole doublet is observed at 4.2°K and 77°K whilst a very small asymmetry (3%) in peak height was ob-

TABLE 9

Mössbauer parameters of some oxo-bridged iron(III) compounds in zero applied magnetic field

Compound	Quadrupole splitting		Isomer shift[a]	
	T (°K)	ΔE (mm.sec^{-1})	δ (mm.sec^{-1})	Ref.
(Fe salen)$_2$O	300	0.92	0.58	27, 105
	77	0.92	0.56	106, 109
				112, 113
(Fe salen)$_2$O.py$_2$	300	0.92	0.71	27
	77	0.88	0.79	
[Fe(sal-N-n-C$_3$H$_7$)$_2$]$_2$O	300	0.94	0.54	[b]
	77	1.04	0.58	
[(Fe phen$_2$Cl)$_2$O]Cl$_2$.5H$_2$O	300	1.70	0.77	27, 81
	77	1.68	0.84	112, 113
[(Fe bipy$_2$)$_2$O](SO$_4$)$_2$3.5H$_2$O	300	1.33	0.73	27, 81
	77	1.51	0.83	
[(Fe terpy)$_2$O](NO$_3$)$_4$.H$_2$O	300	1.93	0.79	27, 81
	77	2.35	0.94	
enH$_2$[(FeHEDTA)$_2$O]6H$_2$O	300	1.69	0.63	79, 109
	77	1.75	0.74	
Na$_4$[(FeEDTA)$_2$O].12H$_2$O	300	1.82	0.66	79
	77	1.94	0.70	
[(FeB(H$_2$O))$_2$O](ClO$_4$)$_4$	300	0.62	0.81	28, 81
	4.2	0.67	0.93	
(FeTPP)$_2$O	300	0.62	0.55	33, 114
(Fe deuteroporph)$_2$O	300	0.64	0.55	31, 114
(Fe protoporph)$_2$O	300	0.66	0.66	114

[a] Relative to sodium nitroprusside.
[b] Unpublished work with A.N. Buckley.

served at 300°K. Below 80°K only the $S' = 0$ pair state is significantly populated and hence there will be no magnetic hyperfine interactions and a symmetric spectrum results; relaxation processes are not relevant[105]. At higher temperatures, $S' \neq 0$ states become populated and their magnetic hyperfine fields can give rise to asymmetry. This asymmetry is very small in (Fe salen)$_2$O since the strong exchange coupling leaves 57% of the $M_{S'} = 0$ states populated at room temperature. In contrast to the weakly coupled analogue (Fe salen Cl)$_2$, the area ratios of the lines are 1.0 at all temperatures, which precludes the presence of any integral asymmetry at high temperatures due to Gol'danskii–Karyagin anisotropic effects (ref. 104, 106). The spectra of [(Fe phen$_2$Cl)$_2$O]Cl$_2$.5H$_2$O appear to show greater relaxation and broadening effects[109].

Applied magnetic-field studies have yielded more detail. Reiff[81] and Okamura et al.[109] have measured spectra at 4°K with applied field strengths of up to 30 kgauss whilst Buckley et al. have used fields of up to 90 kgauss[106]. The spectra for (Fe salen)$_2$O are typical of the

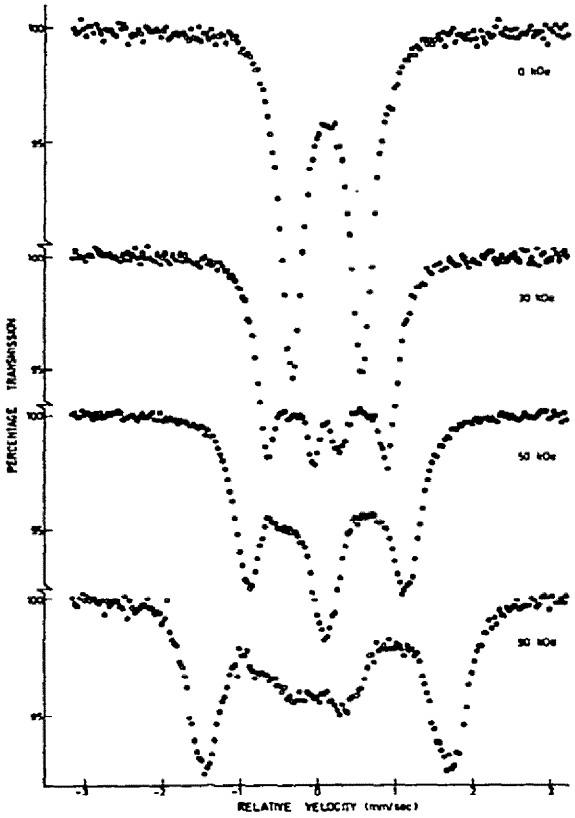

Fig.8. Mössbauer spectra at 4.2°K of (Fe salen)$_2$O in applied magnetic fields.

class and are shown in Fig.8. As the field increases a triplet and doublet appear with overlap of the inner peaks. This behaviour is similar to that calculated by Collins and Travis[110] for the case of no hyperfine magnetic field and random orientation of the electric field gradient (EFG). In this case the principal component of the EFG tensor, V_{zz}, is > 0. The observed field at the iron nuclei is equal to the applied field, which contrasts with the very large hyperfine fields observed at the nuclei of monomeric iron(III) complexes. The spectra are only weakly asymmetric with the asymmetry parameter $\eta = 0.8$. Clear evidence is therefore presented for a spin zero ground state, in agreement with the exchange-coupled model used to describe the present compounds. The spectra of $[(Fe\ phen_2Cl)_2O]Cl_2.5H_2O$, which has ΔE greater than that in the salen case, are better resolved in applied fields[81], and in this case $V_{zz} < 0$ and $\eta \sim 0.2$. $[FeB(H_2O)_2O](ClO_4)_4$ also has $V_{zz} < 0$ but shows an overlapping spectrum[81].

The Mössbauer results, discussed above, have given good correlation with the exchange-coupled $S = \frac{5}{2}$ model, together with considerable findings on relaxation and asymmetry effects. The chemical consequences are minimal, but certain empirical structural and bonding

features can be deduced from consideration of the EFG. Thus, Reiff has concluded that in $[(Fe\ phen_2Cl)_2O]^{2+}$ the Cl and bridging O are *cis* to each other[81]. He proposes that $V_{zz} > 0$ for the salen dimer results from strong σ-bonding in each N_2O_2 ligand plane; a conclusion which differs from the π-bonding argument normally invoked to explain the bonding of O_2 and alkyl groups to metal–salen moieties[111]. In general the polarity and magnitude of V_{zz} and η can be correlated with the environment around the iron atoms known from X-ray studies.

K. ELECTRONIC STRUCTURE OF Fe–O–Fe DIMERS

In the preceding sections F to J we have seen that the model featuring spin–spin coupling of $S = \frac{5}{2}$ iron(III) units gives a particularly good account of electronic ground state properties. The fine structure observed in the single-crystal electronic spectra shows that this model also gives a satisfactory interpretation of associated excited states. Since this model is essentially non-bonding or electrostatic in origin, a better electronic description would be expected to arise from full molecular orbital calculations. Calculations to various degrees of sophistication have been made. The overlap of Fe and O atomic orbitals to explain the superexchange mechanism has already been outlined in Section F. Qualitative three-centre delocalised molecular calculations for a linear M–O–M core have been made by Dunitz and Orgel[115] and later by Jezowska-Trzebiatowska[72]. Octahedral symmetry around the M atom and overall D_{4h} symmetry were assumed. The interaction was assumed to arise only from π-overlap between O($2p_x$, $2p_y$) and M($3d_{xy}$, $3d_{xz}$, $3d_{yz}$) orbitals, which yields the energy levels shown in Fig.9. When the available bonding electrons on M and O are placed in these levels, the diamagnetic ground state of the ten-electron systems Cr–O–Cr and Re–O–Re are predicted correctly ($E_u^4, E_g^4, B_{2g}^2, B_{2u}^0, E_u^{*0}$), but that for Fe–O–Fe is not. In this case, a spin-triplet ground state would be predicted ($\cdots\cdots B_{2u}^2, E_u^{*2}$). Lewis et al. have suggested that the low symmetry of the Fe–O–Fe complexes could possibly cause splitting of the E_u^* level sufficient to cause spin-pairing[20]. They also included a σ-bonding contribution between Fe($3d_{z^2}$) and O($2p_z$) orbitals in the energy level diagram. Jezowska-Trzebiatowska later reached essentially the same conclusions and suggested that the formation of a non-linear Fe–O–Fe bridge is energetically favoured by the electronic splitting of the E_u^* level[72]. She further points out that the filling of E_u^* and higher σ^* orbitals is energetically unfavourable and hence d^6, d^7 and d^8 M–O–M systems should be unstable; this is the case in practice. Application of the angular-overlap method to a linear D_{4h} M–O–M complex yields the same order of energy levels as the σ-modified Dunitz–Orgel scheme[116].

Schugar et al.[79] have recently queried the applicability of the Dunitz–Orgel model in view of their visible spectra results, which show the $^6A_1$ nature of the iron centres, i.e. the $3d$ levels are not significantly affected by oxo-bridge formation. They propose that π-bonding along the Fe–O–Fe unit must involve the empty $4p_\pi$ or $4d_\pi$ orbitals on the metal rather than the $3d$ orbitals. As support for the involvement of outer π orbitals they cite the con-

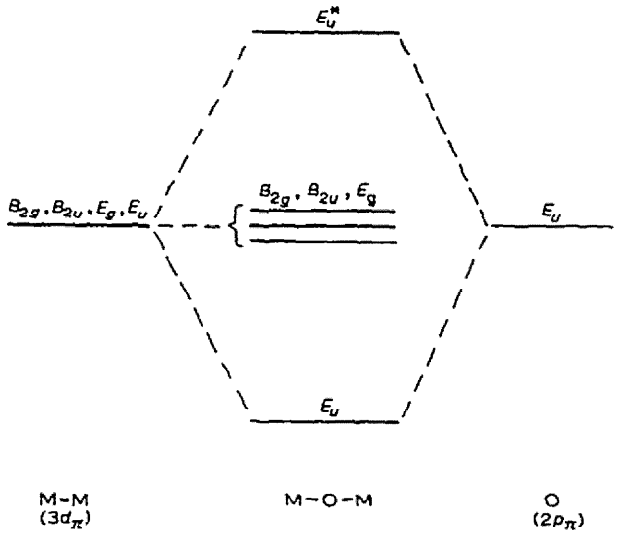

Fig.9. Dunitz–Orgel energy levels for linear M–O–M π-system (not drawn to scale).

stancy of ν(M–O–M) for different metals together with the π-bonding observed in an oxo-bridged Al^{III} dimer (Al–O = 1.68Å)[71].

At this stage of theoretical development, the spin–spin exchange model is ahead of the available molecular-orbital treatments in explaining electronic properties which derive from the 3*d* orbitals. Much more detailed treatments are required to explain properties such as Fe–O–Fe bond lengths and angles, electric-field gradients, spin densities, etc. The use of empty metal π-orbitals by Schugar et al., to explain π-bonding to the bridging oxygen atom, is essentially the argument commonly used to explain d_π–p_π effects in P–O and S–O linkages found in phosphates, sulphates, etc.

L. OXO-BRIDGING IN BIOLOGICAL IRON SYSTEMS

Polynuclear iron clusters are more and more being recognised as important entities in the metal binding sites of a number of proteins and enzymes. Fe–S–Fe bridging has been characterised by X-ray methods in non-haem iron-sulphur proteins[117,118], and exchange interactions across this sulphur bridge have been recognised using magnetic[9,119] and spectroscopic measurements[120–122]. There is less concrete evidence for Fe–O–Fe bridging in native proteins but it seems likely that such is the case in view of its proven existence in a number of model systems.

(i) Haem proteins

(a) Model systems – iron porphyrin complexes

Caughey[30,31,80] and Fleischer[32,53] and their respective co-workers have characterised a

number of oxo-bridged iron(III) complexes with porphyrins such as TPP, deuteroporphyrin IX dimethyl ester and protoporphyrin IX dimethyl ester. X-ray structures have confirmed the binuclearity and Fe–O–Fe bridging[60]. In preliminary stages these compounds were thought by some to have the often-quoted monomeric hydroxo formulation[123,124]. They are synthesised either by autoxidation of iron(II) porphyrins (in solution) or by hydrolysis (aquation) of iron(III) derivatives. Their properties are generally very similar to those of the μ-oxo complexes containing simple ligands, and have already been discussed in detail. It is highly likely that oxo-bridging occurs with porphyrins other than those already studied[114]

(b) Haem proteins

Cytochrome *c* oxidase is considered to possess two haem A groups and two copper atoms at the active site. The mode of oxygen bonding is not yet known. Caughey has shown that Fe–O–Fe bridging exists between haem A groups in the fully oxidised oxidase, despite the large bulky C_{17} side chain on the porphyrin[125]. The NMR spectrum of the oxidase is very similar to that of (Fe protoporph)$_2$O. The copper–iron relationship in this and other[126–128] proteins is a problem of much current interest; in this particular case the possibility of mixed bridging, Cu–O–Fe, has been raised.

Does Fe–O–Fe bridging exist in iron(III) proteins such as haemoglobin, myoglobin, etc.? Hydroxo derivatives have been known for a long time to show magnetic moments reduced from the $S = \frac{5}{2}$ value[129–131]. Magnetic and spectroscopic measurements show fairly conclusively that this behaviour can be explained in terms of a high-spin ($\frac{5}{2}$) $\rightleftharpoons$ low-spin ($\frac{1}{2}$) equilibrium[132–134], i.e. the axial hydroxo ligand creates a crystal field with strength just at the "cross-over" point. The bulky protein chains prevent haem groups coming close together to allow bridging, and a large structural change would be required for this to happen. In the cytochrome *c* oxidase case, discussed above, the haem groups are apparently able to approach each other.

(ii) Haemerythrins

Haemerythrin proteins are involved in oxygen transport in certain invertebrates. The protein, *Golfingia gouldii*, has a molecular weight of 108,000 and is made up of eight sub-units, each of which contains 2 Fe atoms and binds one O_2 molecule. Klotz, Williams and co-workers[109,135,136] and Gray and co-workers[10,137] have recently shown that the active sites in the sub-units of the oxy and met forms consist of exchange-coupled $S = \frac{5}{2}$ iron(III) pairs with Fe–O–Fe bridging. The deoxy form consists of non-bridged high-spin iron(II) moieties. The evidence for a μ-oxo structure is drawn from magnetic[109,137,138], ESR, Mössbauer[109,136,139] and electronic spectral[135,137] measurements; the results are summarised in Table 10. The close similarity to the behaviour of simple dimers is immediately obvious. The reversible oxygenation procedure seems therefore to involve addition of O_2 to two neighbouring deoxy-iron(II) centres to yield the binuclear oxy species. A number of possible structures have been proposed[136,137] for the active site in the oxy form; the magnitude

TABLE 10

Electronic features of oxy- and methaemerythrins

	Oxy-	Met-aquo	Ref.
Magnetism	μ small. $J = -77$ cm^{-1} for $S = \frac{5}{2}$ Fe–Fe pair	μ small. $J = -134$ cm^{-1} for $S = \frac{5}{2}$ Fe–Fe pair. Denatured sample shows $S = \frac{5}{2}$ behaviour.	109, 137, 138
ESR	None	None	135–137
ESR Mössbauer	$\delta = \begin{cases} 0.83 \\ 0.86 \end{cases}$ mm.sec^{-1} $\Delta E = \begin{cases} 1.03 \\ 1.93 \end{cases}$ mm.sec^{-1} Two Fe environments. No broadening at 4.2°K in applied field ∴ diamagnetic ground state	$\delta = 0.81$ mm.sec^{-1}. $\Delta E = 1.57$ mm.sec^{-1}. One Fe environment. No broadening at 4.2°K in applied field ∴ diamagnetic ground state.	109, 136, 139
Electronic	12,990sh (100)	16,670 (100)	135, 137
Spectra, cm^{-1}	20,000 (1200) Fe–O_2 charge transfer	20,410 (290)	
(ϵ per Fe)	27,780sh (2700) 30,300 (3500) Enhanced intensities in visible region due to exchange mechanism	28,170 (3300) Enhanced intensities in visible region due to exchange mechanism	
IR	840 cm^{-1} ν(Fe–O–Fe) ?	840 cm^{-1} ν(Fe–O–Fe) ?	137
Oxidation state	Fe^{III}–peroxo	Fe^{III}	

of J and the non-equivalent iron centres, together with ability to reversibly coordinate oxygen, would possibly favour II or III over I or IV.

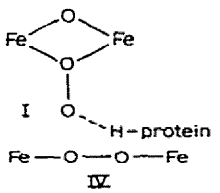

I

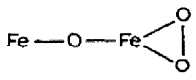

II

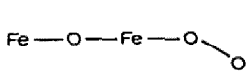

III

IV

The structure of the metaquo species is less ambiguous.

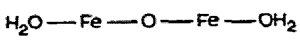

The met form can bind one X group (Cl, N_3, etc.) per iron pair and singly or doubly bridged structures are possible, e.g. for met chlorohaemerythrin

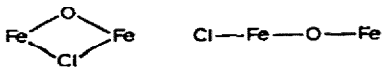

NOTE ADDED IN PROOF

The first example of a binuclear iron complex containing a single sulphur bridge, $(Fesalen)_2S$, has recently been reported[140]. It can be prepared[140] either as a brown precipitate by reacting $Na_2S.H_2O$ with the filtrate obtained from an aqueous B(ii) preparation of $(Fesalen)_2O$, or[141] as small black crystals by reacting Fe(II)salen with sulphur in boiling xylene. The J value, -75 cm^{-1}, is smaller than that of the oxobonded analogue, which is the reverse order to that predicted by simple electronegativity arguments[7]. The Mössbauer parameters, $\Delta E = 0.60$ mm.sec^{-1}; $\delta = 0.68$ mm.sec^{-1}, show a smaller quadruple splitting than for the oxo complex. The complex has possible applications as a model system for the two-iron ferredoxin protein[11].

ACKNOWLEDGEMENTS

The author is indebted to the following colleagues for their efforts in polynuclear iron chemistry: Mr. A. van den Bergen (synthesis); Mr. J.E. Davies and Dr. B.M. Gatehouse (X-ray crystallography); Dr. A.N. Buckley (Mossbauer); Dr. P.D.W. Boyd (NMR); and Dr. L. Dubicki (electronic spectra). In particular, the author would like to thank Professor B.O. West for introducing him to iron chelate chemistry and for continued help and advice.

REFERENCES

1 W.P. Griffith, *Coord. Chem. Rev.*, 5 (1970) 459.
2 A.G. Sykes and J.A. Weil, *Progr. Inorg. Chem.*, 13 (1970) 1.
3 B. Jezowska-Trzebiatowska, *Coord. Chem. Rev.*, 3 (1968) 255; B. Jezowska-Trzebiatowska and W. Wojciechowski, *Transition Metal Chem.*, 6 (1970) 1.
4 S.A. Cotton, *Coord. Chem. Rev.*, 8 (1972) 185.
5 P.W. Ball, *Coord. Chem. Rev.*, 4 (1969) 361.
6 E. Sinn, *Coord. Chem. Rev.*, 5 (1970) 313.
7 R.L. Martin, in E.A.V. Ebsworth, A.G. Maddock and A.G. Sharpe (Eds.), *New Pathways in Inorganic Chemistry*, Cambridge University Press, Cambridge, 1968, p. 175.
8 A.P. Ginsberg, *Inorg. Chim. Acta Rev.*, 5 (1971) 45.
9 J.S. Griffith, *Struct. Bonding (Berlin)*, 10 (1972) 87.
10 T.G. Spiro and P. Saltman, *Struct. Bonding (Berlin)*, 6 (1969) 116.
11 J.C.M. Tsibris and R.W. Woody, *Coord. Chem. Rev.*, 5 (1970) 417.
12 W.R. Dunham, G. Palmer, R.H. Sands and A.J. Bearden, *Biochim. Biophys. Acta*, 253 (1971) 373.
13 H.B. Gray, *Advan. Chem. Ser.*, 100 (1971) 365.
14 P. Pfeiffer, E. Breith, E. Lübbe and T. Tsumaki, *Justus Liebigs Ann. Chem.*, 503 (1933) 84.
15 A. Gaines, L.P. Hammett and G.H. Walden, *J. Amer. Chem. Soc.*, 58 (1936) 1668.
16 W. Klemm and K.H. Raddatz, *Z. Anorg. Chem.*, 250 (1942) 207.
17 A. Bose, *Proc. Indian Acad. Sci., Sect. A*, 1 (1934) 754.
18 A. Earnshaw and J. Lewis, *J. Chem. Soc., London*, (1961) 396.
19 J. Lewis, F.E. Mabbs and A. Richards, *Nature (London)*, 207 (1965) 855.
20 J. Lewis, F.E. Mabbs and A. Richards, *J. Chem. Soc., London*, (1967) 1014.
21 A.V. Khedekar, J. Lewis, F.E. Mabbs and H. Weigold, *J. Chem. Soc., London*, (1967) 1561.
22 L. Michaelis and S. Granick, *J. Amer. Chem. Soc.*, 65 (1943) 481.

23 C.M. Harris and T.N. Lockyer, *Chem. Ind. (London)*, (1958) 1231.
24 N. Elliott, *J. Chem. Phys.*, 35 (1961) 1273.
25 L.N. Mulay and N.L. Hofmann, *Inorg. Nucl. Chem. Lett.*, 2 (1966) 189.
26 G. Anderegg, *Helv. Chim. Acta*, 45 (1962) 1643.
27 W.M. Reiff, W.A. Baker, Jr. and N.E. Erickson, *J. Amer. Chem. Soc.*, 90 (1968) 4794.
28 W.M. Reiff, G.J. Long and W.A. Baker, Jr., *J. Amer. Chem. Soc.*, 90 (1968) 6347.
29 P. Gütlich and B.W. Fitzsimmons, *Angew. Chem., Int. Ed. Engl.*, 8 (1969) 767.
30 J.O. Alben, W.H. Fuchsman, C.A. Beaudreau and W.S. Caughey, *Biochemistry*, 7 (1968) 624.
31 N. Sadasivan, H.I. Eberspaecher, W.H. Fuchsman and W.S. Caughey, *Biochemistry*, 8 (1969) 534.
32 E.B. Fleischer and T.S. Srivastava, *J. Amer. Chem. Soc.*, 91 (1969) 2403.
33 I.A. Cohen, *J. Amer. Chem. Soc.*, 91 (1969) 1980.
34 D.H. Busch, K. Farmery, V. Goldken, V. Katovic, A.C. Melnyk, C.R. Sperati and N. Tokel, *Advan. Chem. Ser.*, 100 (1971) 44.
35 A. van den Bergen, K.S. Murray, M.J.O'Connor, N. Rehak and B.O. West, *Aust. J. Chem.*, 21 (1968) 1505.
36 R.L. Gustafson and A.E. Martell, *J. Phys. Chem.*, 67 (1963) 576.
37 H. Schugar, C. Walling, R.B. Jones and H.B. Gray, *J. Amer. Chem. Soc.*, 89 (1967) 3712.
38 H.B. Gray, *Rec. Chem. Progr.*, 29 (1968) 163.
39 J.D. Curry and D.H. Busch, *J. Amer. Chem. Soc.*, 86 (1964) 592.
40 A. van den Bergen and K.S. Murray, unpublished result.
41 S.M. Crawford, *Spectrochim. Acta*, 19 (1963) 255.
42 R.N. Sylva, *Rev. Pure Appl. Chem.*, 22 (1972) 115.
43 C.L. Rollinson, in J.C. Bailar, Jr. (Ed.), *Chemistry of the Coordination Compounds*, Reinhold, New York, 1956, p. 448.
44 G. Jander and J. Jahr, *Kolloid-Beih.*, 43 (1936) 305, 323.
45 H. Wendt, *Inorg. Chem.*, 8 (1969) 1527.
46 B. Lutz and H. Wendt, *Ber. Bunsenges. Phys. Chem.*, 74 (1970) 372.
47 B.A. Sommer and D.W. Margerum, *Inorg. Chem.*, 9 (1970) 2517.
48 T.J. Connocchioli, E.J. Hamilton and N. Sutin, *J. Amer. Chem. Soc.*, 87 (1965) 926.
49 H.N. Po and N. Sutin, *Inorg. Chem.*, 10 (1971) 428.
50 L.N. Mulay and P.W. Selwood, *J. Amer. Chem. Soc.*, 77 (1955) 2693.
51 R.G. Wilkins and R.E. Yelin, *Inorg. Chem.*, 8 (1969) 1470.
52 H.J. Schugar, A.T. Hubbard, F.C. Anson and H.B. Gray, *J. Amer. Chem. Soc.*, 90 (1969) 71.
53 E.B. Fleischer, J.M. Palmer, T.S. Srivastava and A. Chatterjee, *J. Amer. Chem. Soc.*, 93 (1971) 3162.
54 H.J. Schugar, G.R. Rossman and H.B. Gray, *J. Amer. Chem. Soc.*, 91 (1969) 4564.
55 I.A. Cohen and W.S. Caughey, *Biochemistry*, 7 (1968) 636.
56 E.B. Fleischer and S. Hawkinson, *J. Amer. Chem. Soc.*, 89 (1967) 720.
57 J.E. Davies and B.M. Gatehouse, unpublished data.
58 M. Gerloch, E.D. McKenzie and A.D.C. Towl, *J. Chem. Soc. A*, (1969) 2850.
59 P. Coggon, A.T. McPhail, F.E. Mabbs and V.N. McLachlan, *J. Chem. Soc. A*, (1971) 1014.
60 L.O. Atovmyan, O.A. D'yachenko and S.V. Soboleva, *J. Struct. Chem. (USSR)*, 11 (1970) 517.
61 A.B. Hoffman, D.M. Collins, V.W. Day, E.B. Fleischer, T.S. Srivastava and L.H. Hoard, *J. Amer. Chem. Soc.*, 94 (1972) 3620.
62 S.J. Lippard, H.J. Schugar and C. Walling, *Inorg. Chem.*, 6 (1967) 1825.
63 J.E. Davies and B.M. Gatehouse, *Cryst. Struct. Commun.*, 1 (1972) 115.
64 J.E. Davies and B.M. Gatehouse, unpublished data.
65 M. Yewitz and J.A. Stanko, *J. Amer. Chem. Soc.*, 93 (1971) 1512.
66 A. Urushiyama, T. Nomura and M. Nakahara, *Bull. Chem. Soc. Jap.*, 43 (1970) 3971; 45 (1972) 2406.
67 E. Pedersen, *Acta Chem. Scand.*, 26 (1972) 333.
68 L.H. Vogt, A. Zalkin and D.H. Templeton, *Inorg. Chem.*, 6 (1967) 127.
69 J.C. Morrow, *Acta Crystallogr.*, 15 (1962) 851.
70 A.M. Matheson, D.P. Mellor and N.C. Stephenson, *Acta Crystallogr.*, 5 (1952) 185.

71 Y. Kushi and Q. Fernando, *J. Amer. Chem. Soc.*, 92 (1970) 91.
72 B. Jezowska-Trzebiatowska, *Pure Appl. Chem.*, 27 (1971) 89.
73 D.J. Hewkin and W.P. Griffith, *J. Chem. Soc. A*, (1966) 474.
74 R. Driver and W.R. Walker, *Aust. J. Chem.*, 20 (1967) 1375.
75 W. Heisenberg, *Z. Phys.*, 38 (1926) 411; 49 (1928) 619.
76 P.A.M. Dirac, *Proc. Roy. Soc. A*, 123 (1929) 714.
77 J.H. Van Vleck, *The Theory of Electric and Magnetic Susceptibilities*, Oxford University Press, Oxford, 1932 Chap. XII.
78 A. van den Bergen, K.S. Murray and B.O. West, *Aust. J. Chem.*, 21 (1968) 1517.
79 H.J. Schugar, G.R. Rossman, C.G. Barraclough and H.B. Gray, *J. Amer. Chem. Soc.*, 94 (1972) 2683.
80 T.H. Moss, H.P. Lillienthal, C. Moleski, G.A. Smythe, M.C. McDaniel and W.S. Caughey, *Chem. Commun.*, (1972) 263.
81 W.M. Reiff, *J. Chem. Phys.*, 54 (1971) 4718.
82 F.A. Cotton and G. Wilkinson, *Advanced Inorganic Chemistry*, 3rd edn., Interscience, New York, 1972, p.866.
83 P.W. Anderson, *Solid State Phys.*, 14 (1963) 99.
84 J.B. Goodenough, *Magnetism and the Chemical Bond*, Interscience, New York, 1963, Chap. II.
85 J.S. Griffith, *Proc. Roy. Soc., Ser. A*, 235 (1956) 23.
86 M. Gerloch and P.N. Quested, *J. Chem. Soc. A*, (1971) 2307.
87 D.J. Brown, M. Gerloch and J. Lewis, *Nature (London)*, 220 (1968) 256.
88 J.E. Davies and K.S. Murray, unpublished results.
89 M.Y. Okamura and B.M. Hoffman, *J. Chem. Phys.*, 51 (1969) 3128.
90 K.S. Murray, unpublished results.
91 J. Ferguson, H.J. Guggenheim and Y. Tanabe, *J. Phys. Soc. Jap.*, 21 (1966) 692.
92 L. Dubicki, *Aust. J. Chem.*, 25 (1972) 1141.
93 L. Dubicki and D. Schulberg, unpublished results.
94 J. Ferguson and P.E. Fielding, *Aust. J. Chem.*, 25 (1972) 1371.
95 P.D.W. Boyd and K.S. Murray, *J. Chem. Soc. A*, (1971) 2711.
96 B.R. McGarvey and R.J. Kurland, *J. Magn. Res.*, 2 (1970) 286.
97 M. Wicholas, R. Mustacich and D. Jayne, *J. Amer. Chem. Soc.*, 94 (1972) 4518.
98 P.D.W. Boyd and T.D. Smith, *Inorg. Chem.*, 10 (1971) 2041.
99 G. La Mar, G.R. Eaton, R.H. Holm and F.A. Walker, *J. Amer. Chem. Soc.*, 95 (1973) 63.
100 R.L. Martin, R.M. Golding, W.C. Tennant, C.R. Kanekar and A.H. White, *J. Chem. Phys.*, 45 (1966) 2688.
101 R.H. Holm, *Accounts Chem. Res.*, 2 (1969) 307.
102 M. Wicholas, *J. Amer. Chem. Soc.*, 92 (1970) 4141.
103.M. Wicholas and D. Jayne, *Inorg. Nucl. Chem. Lett.*, 7 (1971) 443.
104 A.N. Buckley, G.V.H. Wilson and K.S. Murray, *Solid State Commun.*, 7 (1969) 471.
105 A.N. Buckley, G.V.H. Wilson and K.S. Murray, *Chem. Commun.*, (1969) 718.
106 A.N. Buckley, I.R. Herbert, B.D. Rumbold, G.V.H. Wilson and K.S. Murray, *J. Phys. Chem. Solids*, 31 (1970) 1423.
107 A.N. Buckley, B.D. Rumbold, G.V.H. Wilson and K.S. Murray, *J. Chem. Soc. A*, (1970) 2298.
108 M. Cox, B.W. Fitzsimmons, A.W. Smith, L.F. Larkworthy and K.A. Rogers, *Chem. Commun.*, (1969) 183.
109 M.Y. Okamura, I.M. Klotz, C.E. Johnson, M.R.C. Winter and R.J.P. Williams, *Biochemistry*, 8 (1969) 1951.
110 R.L. Collins and J.C. Travis, *Möessbauer Eff. Methodol., Proc. Symp.*, 3 (1967) 123.
111 H.A.O. Hill, J.M. Pratt and R.J.P. Williams, *Discuss. Faraday Soc.*, 47 (1969) 165.
112 R.R. Berrett, B.R. Fitzsimmons and A.A. Owusu, *J. Chem. Soc. A*, (1968) 1575.
113 G.M. Bancroft, A.G. Maddock and R.P. Randl, *J. Chem. Soc. A*, (1968) 2939.
114 (a) M.A. Torrens, D.K. Straub and L.M. Epstein, *J. Amer. Chem. Soc.*, 94 (1972) 4100; (b) W. Karger, *Ber. Bunsenges. Phys. Chem.*, 68 (1964) 79.
115 J. Dunitz and L.E. Orgel, *J. Chem. Soc., London*, (1953) 2594.

116 H.H. Schmidtke, *Theor. Chim. Acta*, 20 (1971) 92.
117 L.C. Sieker, E. Adman and L.H. Jensen, *Nature (London)*, 235 (1972) 40.
118 C.W. Carter, S.T. Freer, Ng.H. Xuong, R.A. Alden and J. Kraut, *Cold Spring Harbor Symp. Quant. Biol.*, 36 (1971) 381.
119 T.H. Moss, D. Petering and G. Palmer, *J. Biol. Chem.*, 244 (1969) 227.
120 M. Poe, W.D. Phillips, J.D. Glickson, C.C. McDonald and A. San Pietro, *Proc. Nat. Acad. Sci. U. S. A.*, 68 (1971) 68.
121 A.J. Bearden and W.R. Dunham, *Struct. Bonding (Berlin)*, 8 (1970) 1.
122 L.N. Kramer and M.P. Klein, in D.A. Shirley (Ed.), *Electron Spectroscopy*, North-Holland, Amsterdam, 1972, p.733.
123 C. Maricondi, W. Swift and D.K. Straub, *J. Amer. Chem. Soc.*, 91 (1969) 5205.
124 E.B. Fleischer and C.K. Miller, *J. Amer. Chem. Soc.*, 86 (1964) 2342.
125 W.S. Caughey, *Advan. Chem. Ser.*, 100 (1971) 248.
126 E. Frieden, *Advan. Chem. Ser.*, 100 (1971) 292.
127 B.F. van Gelder and H. Beinert, *Biochem. Biophys. Acta*, 189 (1969) 1.
128 J.S. Griffith, *Mol. Phys.*, 21 (1971) 141.
129 C.D. Coryell, F. Stitt and L. Pauling, *J. Amer. Chem. Soc.*, 59 (1937) 633.
130 W.A. Rawlinson, *Aust. J. Exp. Biol. Med. Sci.*, 18 (1940) 185.
131 J.E. Falk, *Porphyrins and Metalloporphyrins*, Elsevier, Amsterdam, 1964.
132 R.L. Martin and A.H. White, *Transition Metal Chem.*, 4 (1968) 113.
133 D.W. Smith and R.J.P. Williams, *Struct. Bonding (Berlin)*, 7 (1970) 1.
134 M. Weissbluth, *Struct. Bonding, (Berlin)*, 2 (1967) 1.
135 K. Garbett, D.W. Darnell, I.M. Klotz and R.J.P. Williams, *Arch. Biochem. Biophys.*, 135 (1969) 419.
136 K. Garbett, C.E. Johnson, I.M. Klotz, M.Y. Okamura and R.J.P. Williams, *Arch. Biochem. Biophys.*, 142 (1971) 574.
137 J.W. Dawson, H.B. Gray, H.E. Hoenig, G.R. Rossman, J.M. Schredder and R.H. Wang, *Biochemistry*, 11 (1972) 461.
138 T.H. Moss, C. Moleski and J.L. York, *Biochemistry*, 10 (1971) 840.
139 J.L. York and A.J. Bearden, *Biochemistry*, 9 (1970) 4549.
140 P.C.H. Mitchell and D.A. Parker, *J. Inorg. Nucl. Chem.*, 35 (1973) 1385.
141 A. van den Bergen, K.S. Murray and B.O. West, unpublished results.